



# **International Ocean Discovery Program**

## **Expedition 395E Preliminary Report**

### **Complete South Atlantic Transect Reentry Systems**

**6 April–5 June 2021**

Trevor Williams, Emily R. Estes, Bill Rhinehart, Rosalind M. Coggon, Jason B. Sylvan, Gail L. Christeson, and Damon A.H. Teagle

## Publisher's notes

Core samples and the wider set of data from the science program covered in this report are under moratorium and accessible only to Science Party members until 7 February 2024.

This publication was prepared by the *JOIDES Resolution* Science Operator (JRSO) at Texas A&M University (TAMU) as an account of work performed under the International Ocean Discovery Program (IODP). This material is based upon work supported by the JRSO, which is a major facility funded by the National Science Foundation Cooperative Agreement Number OCE1326927. Funding for IODP is provided by the following international partners:

National Science Foundation (NSF), United States  
Ministry of Education, Culture, Sports, Science and Technology (MEXT), Japan  
European Consortium for Ocean Research Drilling (ECORD)  
Ministry of Science and Technology (MOST), People's Republic of China  
Korea Institute of Geoscience and Mineral Resources (KIGAM)  
Australia-New Zealand IODP Consortium (ANZIC)  
Ministry of Earth Sciences (MoES), India

Portions of this work may have been published in whole or in part in other IODP documents or publications.

## Disclaimer

The JRSO is supported by the NSF. Any opinions, findings, and conclusions or recommendations expressed in this material do not necessarily reflect the views of the NSF, the participating agencies, TAMU, or Texas A&M Research Foundation.

## Copyright

Except where otherwise noted, this work is licensed under the Creative Commons Attribution 4.0 International (CC BY 4.0) license (<https://creativecommons.org/licenses/by/4.0/>). Unrestricted use, distribution, and reproduction are permitted, provided the original author and source are credited.



## Citation

Williams, T., Estes, E.R., Rhinehart, B., Coggon, R.M., Sylvan, J.B., Christeson, G.L., and Teagle, D.A.H., 2021. *Expedition 395E Preliminary Report: Complete South Atlantic Transect Reentry Systems*. International Ocean Discovery Program. <https://doi.org/10.14379/iodp.pr.395E.2021>

## ISSN

World Wide Web: 2372-9562

## Expedition 395E participants

### Expedition 395E scientists (shore based)

#### Trevor Williams

##### Expedition Project Manager/Staff Scientist Expedition 393/395E

International Ocean Discovery Program  
Texas A&M University  
USA  
[williams@iodp.tamu.edu](mailto:williams@iodp.tamu.edu)

#### Emily R. Estes

##### Expedition Project Manager/Staff Scientist Expedition 390/390C

International Ocean Discovery Program  
Texas A&M University  
USA  
[estes@iodp.tamu.edu](mailto:estes@iodp.tamu.edu)

#### Rosalind M. Coggon

##### Co-Chief Scientist Expedition 390

School of Ocean and Earth Science  
University of Southampton  
United Kingdom  
[R.M.Coggon@soton.ac.uk](mailto:R.M.Coggon@soton.ac.uk)

#### Jason B. Sylvan

##### Co-Chief Scientist Expedition 390

Department of Oceanography  
Texas A&M University  
USA  
[jasonsylvan@tamu.edu](mailto:jasonsylvan@tamu.edu)

#### Gail L. Christeson

##### Co-Chief Scientist Expedition 393

Institute for Geophysics  
University of Texas at Austin  
USA  
[gail@ig.utexas.edu](mailto:gail@ig.utexas.edu)

#### Damon A.H. Teagle

##### Co-Chief Scientist Expedition 393

School of Ocean and Earth Science  
University of Southampton  
United Kingdom  
[Damon.Teagle@southampton.ac.uk](mailto:Damon.Teagle@southampton.ac.uk)

## Operational and technical staff

### Siem Offshore AS officials

#### Jake Robinson

Master of the Drilling Vessel

#### Mark Robinson

Drilling Supervisor

### JRSO shipboard personnel and technical representatives

#### Alejandro Avila Santis

Physical Properties Laboratory

#### Carel Lewis

Curatorial Specialist

#### Susan Boehm

Thin Section Laboratory

#### Daniel Marone

Downhole Tools/Underway Geophysics Laboratory

#### James Brattin

Applications Developer

#### Aaron Mechler

Chemistry Laboratory

#### Aaron de Loach

Assistant Laboratory Officer

#### Beth Novak

Assistant Laboratory Officer

#### Clayton Furman

Logging Engineer (Schlumberger)

#### Bill Rhinehart

Operations Superintendent

#### Randy Gjesvold

Marine Instrumentation Specialist

#### Alyssa Stephens

Marine Laboratory Specialist

#### Sandra Herrmann

Imaging Specialist

#### Brittany Stockmaster

Marine Laboratory Specialist

#### Mark Higley

Paleomagnetism Laboratory

#### Steven Thomas

Marine Computer Specialist

#### Michael Hodge

Marine Computer Specialist

## 1. Abstract

International Ocean Discovery Program (IODP) Expeditions 390C and 395E were implemented in response to the global COVID-19 pandemic and occupied sites proposed for the postponed Expeditions 390 and 393, South Atlantic Transect 1 and 2. Expedition 395E completed most of the preparatory work that Expedition 390C did not have time to complete. The overall objective of Expeditions 390C and 395E was to core one hole at each of the South Atlantic Transect sites with the advanced piston corer/extended core barrel (APC/XCB) system to basement for gas safety monitoring and to install a reentry system with casing through the sediment to a few meters into basement in a second hole.

Expedition 395E started in Cape Town, South Africa, and ended in Reykjavík, Iceland, after 20 days of on-site operations. We cored to basement at two new sites, U1560 and U1561, and completed reentry systems at three sites, U1556, U1557, and U1560. These operations will expedite basement drilling during the rescheduled Expeditions 390 and 393.

Hole U1560A (Proposed Site SATL-25A) lies in ~15.2 Ma crust and is composed of carbonate-rich sediments to 120 meters below seafloor (mbsf) and 2.5 m of underlying basalt. A reentry system was deployed in Hole U1560B to 122.0 mbsf. We then moved to the sites at the western end of the transect on ~61 Ma crust. In Hole U1557D, 10% inch casing was deployed to 571.6 mbsf to deepen the 16 inch casing that was deployed during Expedition 390C, and in Hole U1556B, a reentry system was deployed to 284.2 mbsf. The remaining operations time was insufficient to install a reentry system at the originally planned site, Proposed Site SATL-33B. Instead, we cored Hole U1561A (Proposed Site SATL-55A) to 47 mbsf. It is composed of red clay and carbonate ooze overlying 3 m of basalt.

The six primary sites of the South Atlantic Transect lie perpendicular to the Mid-Atlantic Ridge on the South American plate, overlying crust ranging in age from 7 to 61 Ma. Basement coring will increase our understanding of how crustal alteration progresses over time across the flanks of a slow/intermediate-spreading ridge and how microorganisms survive in deep subsurface environments. Sediment will be used in paleoceanographic and microbiological studies.

## 2. Introduction

In 2020 and 2021, the global COVID-19 pandemic resulted in the postponement of several International Ocean Discovery Program (IODP) expeditions, chiefly because science parties were unable to travel to the ship. In response, the ship was used to conduct preparatory work for the postponed expeditions that did not require a science party aboard but could be carried out by the ship's crew and a team of technicians from the *JOIDES Resolution* Science Operator (JRSO). Two of these expeditions were in service of IODP South Atlantic Transect (SAT) Expeditions 390 and 393. The first was Expedition 390C, which sailed in October–November 2020 (Estes et al., 2021). The second was Expedition 395E, the subject of this report.

Four of the SAT sites (U1556–U1559) were cored during Expedition 390C. However, there were difficulties installing casing into basement because Dril-Quip running tools were found to be incompatible with use in hard rock. The release mechanism does not work when the casing string weight cannot be fully removed from the running tool, which can happen when the base of casing is in basement. Therefore, at Sites U1558 and U1559, casing was installed to ~10 m above basement rather than a few meters into basement as planned. Site U1557 has a thick sediment cover (564 m), and a 16 inch casing string was installed to 60 meters below seafloor (mbsf) at this site. The extra time taken for troubleshooting meant that reentry installations could not be completed at the other sites, and a second expedition was planned.

IODP Expedition 395P (4 February–6 April 2021) was given the go-ahead by the *JOIDES Resolution* Facility Board to complete the reentry system installations without a science party. Unfortunately, Expedition 395P did not leave port in Cape Town, South Africa, because of COVID-19 cases among the staff and crew in the port call hotel and on the ship. Its operations were deferred to Expedition 395E, which started in Cape Town on 6 April and ended on 6 June 2021 in Reykjavík,

Iceland. Operations time was limited to 20 days because of the 3 week transit to Reykjavík at the end of the expedition.

The objectives for Expedition 395E were to core and install reentry systems at the remaining SAT sites. Coring one hole at each site was necessary to establish the depth to basement and for gas safety monitoring. We used the advanced piston corer/extended core barrel (APC/XCB) system, and all rotary core barrel (RCB) drilling was deferred to Expeditions 390 and 393. The APC/XCB cores recovered during Expedition 395E will be considered part of Expeditions 390 and 393 for use by their science parties.

Having reentry systems in place at each site decreases the operational risk of the SAT expeditions and better guarantees that we recover the basement material needed to achieve the science objectives. The reentry systems were to be installed with the hydraulic release tool (HRT), except for Hole U1557D, where we used a Dril-Quip to be compatible with the existing reentry hardware. We aimed to place the bottom of casing up to 5 m into basement to make a more stable hole for basement coring than if the sometimes unstable top of basement is left uncased. However, this was not always possible because of local seafloor and basement surface topography.

Expeditions 390 and 393 will recover sedimentary sections and the upper ~250 m of underlying ocean crust at six sites along a slow/intermediate spreading rate Mid-Atlantic Ridge (MAR) crustal flow line at ~31°S (Figure F1). The expeditions will operate in a region last visited during Deep Sea Drilling Project (DSDP) Leg 3, which helped verify theories of seafloor spreading and plate tectonics. After 50 y of advances in drilling technologies and analytical capabilities, we expect that a new transect will result in significant interdisciplinary contributions to our understanding of Earth processes. Transects of drill holes that sample both the sediment cover and the uppermost oceanic crust in a particular ocean basin can provide essential knowledge of how interconnected processes have evolved over Earth's history and responded to changes in external drivers such as atmospheric CO<sub>2</sub> concentrations, oceanic gateways, or major ocean currents. Transects that sample tens of millions of years of ocean crust formed at the same mid-ocean ridge (MOR) can provide important information about the duration of hydrothermal exchange. However, sampling both the sediment and the underlying basaltic basement in a specific ocean region has rarely been undertaken in a systematic manner, and the few transects accomplished cover relatively short intervals of Earth history (e.g., Juan de Fuca Ridge, 0–3.5 Ma [Shipboard Scientific Party, 1997; Expedition 301 Scientists, 2005; Expedition 327 Scientists, 2011], and Costa Rica Rift, 0–7 Ma [Anderson, Honnorez, Becker, et al., 1985]).

On average, there is a discernible conductive heat flow deficit out to 65 Ma crust (e.g., Stein and Stein, 1994), indicating that there is significant advection of heat from the cooling of the oceanic lithosphere out to this age. However, basement hydrological flow can occur in crust of all ages if sufficient hydrologic heads can be established because crustal age is only one of a suite of inter-linked parameters that influence the duration, depth, and intensity of off-axis hydrothermal fluid flow. Other key parameters include spreading rate, basement roughness, volcanic stratigraphy, and flow morphology as well as sediment type, thickness, and completeness of basement blanketing. Simple relationships may not exist between crustal age, fluid flow, thermal and chemical exchange, and biological activity. Figure F2 summarizes potential relationships between these parameters.

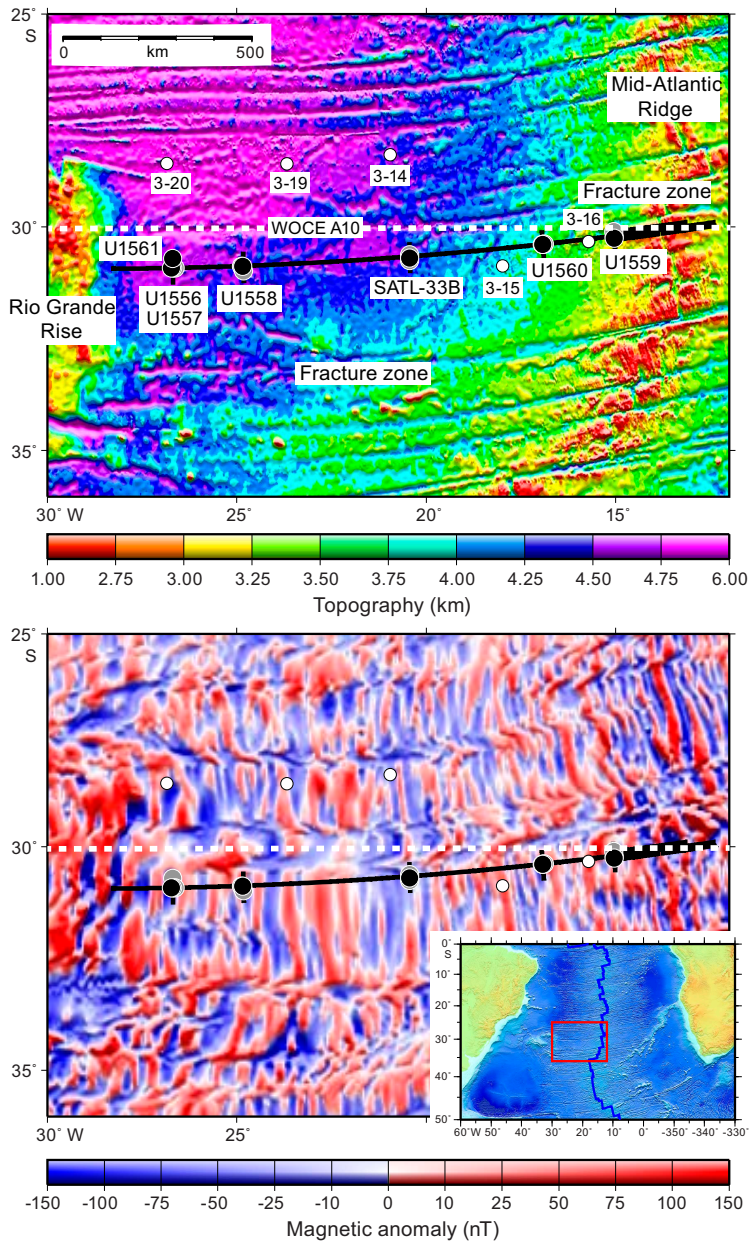


**Figure F1.** South Atlantic Transect study region. Top: bathymetry (Ryan et al., 2009). Bottom: magnetic anomalies (Maus et al., 2009). Inset shows regional setting. Black lines = Crustal Reflectivity Experiment Southern Transect (CREST) seismic reflection profiles, white dashed line = World Ocean Circulation Experiment (WOCE) Line A10. Expedition 390C, 390, and 393 sites are displayed with black (primary) and gray (alternate) dots. White dots = DSDP Leg 3 sites.

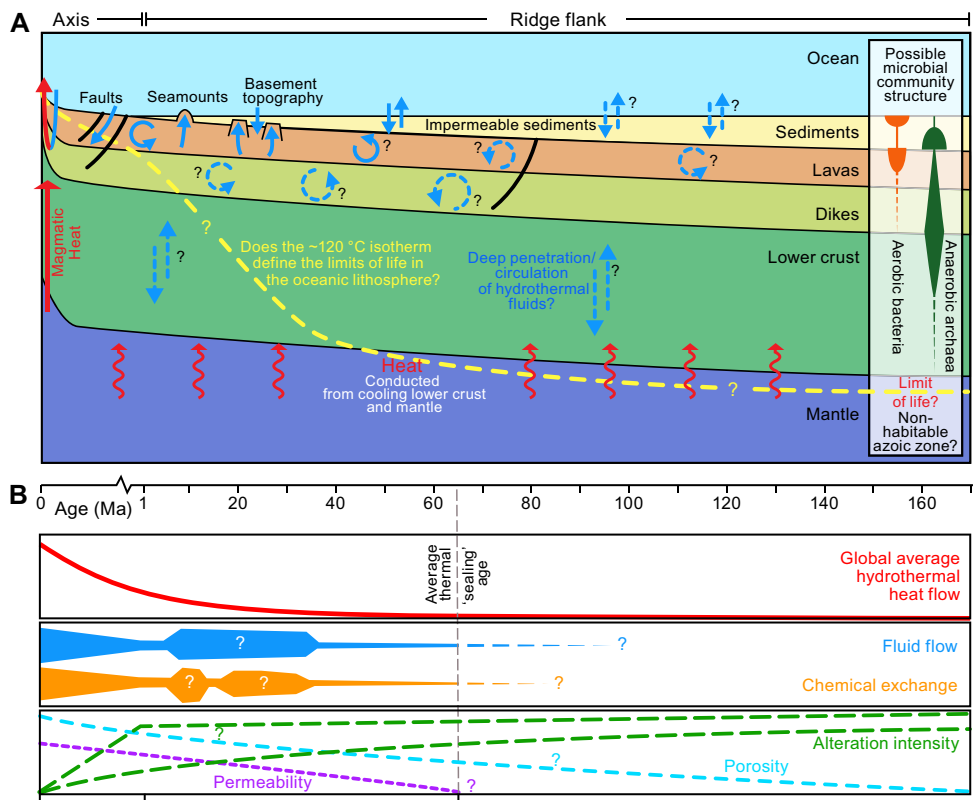


**Figure F2.** A. Schematic architecture of a mid-ocean ridge flank (not to scale) illustrating parameters that may influence intensity and style of hydrothermal alteration and hypothetical trajectory of 120°C isotherm with crustal age. Arrows indicate heat (red) and fluid (blue) flow. B. Calculated global hydrothermal heat flow anomaly, which decreases to 0 by 65 Ma on average, and hypothetical variations in fluid flow and chemical exchange and crustal properties that could be measured to investigate intensity and style of ridge flank hydrothermal circulation (e.g., porosity, permeability, and two possible scenarios for alteration intensity). (After Coggon and Teagle, 2011; Expedition 335 Scientists, 2012; and an original figure by K. Nakamura, AIST.)

### 3. Background

#### 3.1. Geological setting

Expeditions 390 and 393 will operate along a transect at ~31°S just south of the Leg 3 transect (~28.5°S). The new transect was selected with sites that will (1) target basement formed along the same crustal flow line at similar rates (~13–25 mm/y half rate) (Table T1) and (2) recover sections of slow-spreading crust of comparable ages to the ocean crust reference sections in Ocean Drilling Program (ODP) Holes 504B (7 Ma) (Shipboard Scientific Party, 1993) and 1256D (15 Ma) (Shipboard Scientific Party, 2003; Expedition 309/312 Scientists, 2006; Expedition 335 Scientists, 2012), which are located in intermediate- and superfast-spreading crust, respectively. The site locations were chosen to optimize recovery of material required to achieve multidisciplinary objectives. Thicker sediment layers are frequently targeted by scientific drilling to maximize the resolution of paleoceanographic records. However, this decision has biased our sampling of in situ upper ocean crust to regions with thick sedimentary cover (for holes that penetrate >100 m into basement), which drilling as part of the SAT expeditions seeks to remediate (Figure F3). Rapid deposition of sediment seals crust off from the oceans, resulting in anomalously hot basement temperatures and potentially causing premature cessation of hydrothermal circulation. Consequently, most SAT target sites have sediment cover that is close to the global average thickness for their crustal age (Spinelli et al., 2004). However, because seafloor roughness is greater in slow-spreading ocean basins than in fast-spreading basins (Spinelli et al., 2004), there are significant variations in sediment thickness and the continuity of coverage along the transect. Basement crops out at all ages along the transect (Estep et al., 2019) (Figure F4), and these topographic variations likely impact the

crustal hydrogeology. Two sites lie ~6.7 km apart on crust estimated to be 61 Ma; crust at Site U1556 underlies 278 m of sediment, and Site U1557 (Proposed Site SATL-56A) basalts underlie 564 m of sediment.

The 15 Ma site (U1560, Proposed Site SATL-25A) was chosen for comparison to Hole 1256D (Shipboard Scientific Party, 2003; Expedition 309/312 Scientists, 2006; Expedition 335 Scientists, 2012). The sediment sections cored at the 61 Ma sites (U1556 and U1557) are expected to capture key Paleogene hyperthermals, including the Paleocene/Eocene Thermal Maximum (PETM), and the underlying basement will record the cumulative hydrothermal alteration of the uppermost crust across the entire SAT. Another 61 Ma site (U1561, Proposed Site SATL-55A) provides a thinner sediment alternate to Site U1556. The 7 Ma site (U1559) provides the young end-member for investigating the evolution of hydrothermal and microbiological systems with crustal age and allows comparison with similar-aged intermediate-spreading rate crust from Hole 504B (Shipboard Scientific Party, 1993). The 31 Ma (Proposed Site SATL-33B) and 49 Ma (Site U1558) sites fill critical gaps in our ocean crust and deep biosphere sampling with respect to basement age and major changes in ocean chemistry (Coggon et al., 2010).

Leg 3 drilling results provide an indication of what to expect in the sedimentary columns of the SAT sites (Scientific Party, 1970). During Leg 3, 10 sites were drilled in the equatorial and South Atlantic Ocean between Senegal and Brazil, including 7 sites along a transect across the MAR that penetrated to basement (DSDP Sites 14–20). The basal sediment ages were within a few million years of the inferred magnetic anomaly ages, which is consistent with a half spreading rate of ~20 mm/y since 76 Ma. Recovery in the cored intervals was typically high (>98%), but the sediments were only spot cored, and there are significant gaps between cored intervals. The recovered cores make up an almost continuous Lower Cretaceous to Pleistocene composite stratigraphic section.

**Table T1.** Site background information updated based on Expedition 390C and 395E findings. NA = not applicable, sites were not visited.

Expedition	Site	Hole	Age (Ma)	Half-spreading rate (mm/y)	Estimated sediment thickness (mbsf)	Observed sediment thickness (mbsf)	Average sediment accumulation rate (m/My)	Total penetration (m)
390C	U1556	A	61.2	13.5	180	278.0	4.54	283.8
390C	U1557	B	61.2	13.5	510	564.0	9.22	574.0
395E	U1561	A	61.2	13.5	126	46.0	0.75	49.0
390C	U1558	A	49.2	19.5	148	158.9	3.23	163.9
NA	SATL-33B	NA	30.6	24.0	138	NA	4.51	NA
395E	U1560	A	15.2	25.5	104	120.0	6.84	122.5
390C	U1559	A	6.6	17.0	50	64.0	9.70	66.2

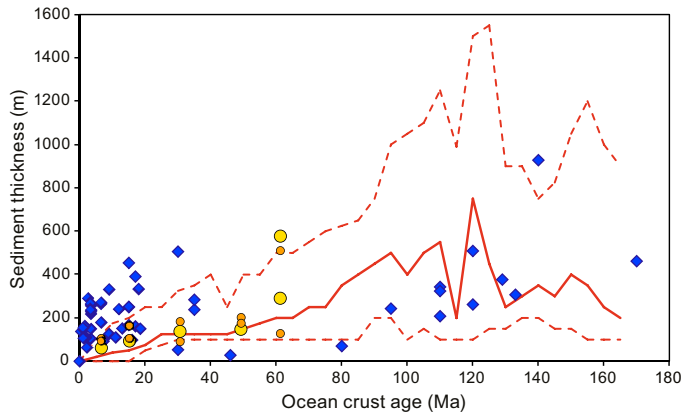


**Figure F3.** Sediment cover vs. crustal age for Expedition 390C, 390, 393, and 395E primary (yellow) and alternate (orange) sites. Blue diamond = sediment thicknesses at all DSDP/ODP/Integrated Ocean Drilling Program/IODP drill holes that cored more than 100 m into basement of intact oceanic crust and tectonically exposed lower crust/upper mantle. Red line = global average sediment thickness vs. age (red dashed lines =  $\pm 1\sigma$  variation) (after Spinelli et al., 2004).

All sites yielded calcareous sediments with calcareous nannoplankton and planktonic foraminifera.

### 3.2. Seismic studies/site survey data

The SAT is located along a crustal flow line where fracture zones are far apart, magnetic lineations are clear, and there is little disruption in seafloor bathymetry (Figure F1). The Crustal Reflectivity Experiment Southern Transect (CREST) cruise aboard the research vessel (R/V) *Marcus G. Langseth* in January and February 2016 conducted a detailed geophysical survey (<https://doi.org/10.1594/IEDA/500255>) of the area, including a 1500 km multichannel seismic reflection profile from the ridge crest to the Rio Grande Rise spanning 0–70 Ma crust, two shorter ridge-crossing profiles spanning 0–7 Ma crust, and five ridge-parallel profiles. Ocean bottom seismometer profiles were acquired coincident with the ridge-parallel profiles. Gravity, magnetics, multibeam bathymetry, and backscatter data were also acquired. Figure F4 shows seismic reflection profiles for Expedition 395E sites.

The present-day MAR axis at 30°–32°S has a well-defined axial valley with two inferred active hydrothermal vents (Schmid et al., 2019). The CREST seismic survey crossed a ridge segment that is ~100 km long and bounded to the north and south by ridge offsets ~16 to ~22 km in width. The

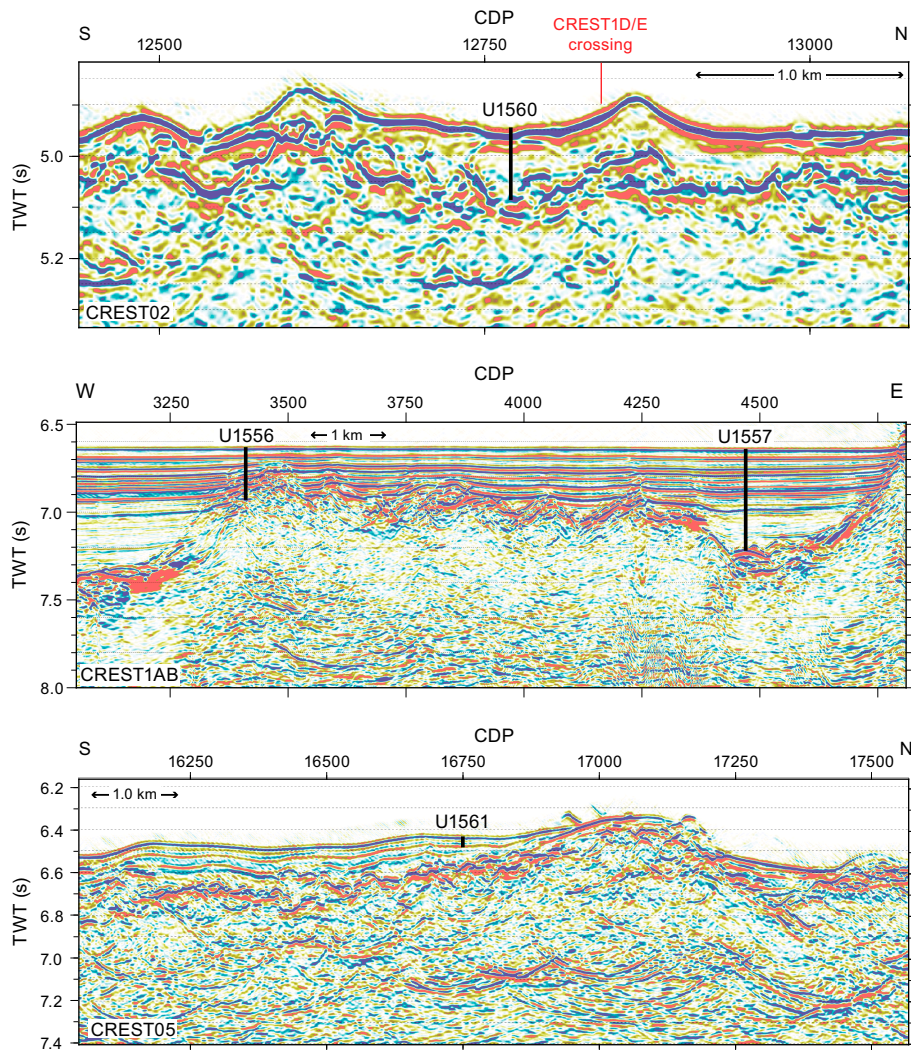


**Figure F4.** Seismic reflection profiles for Expedition 395E sites. Sites U1560 and U1561 were cored and Sites U1556 and U1557 were cased during this expedition, having been cored during Expedition 390C. Black lines = cored depth. TWT = two-way traveltime, CDP = common depth point.

absence of domal structures, which would represent oceanic core complexes (OCCs) formed by detachment faulting, near the ridge axis and the well-defined marine magnetic anomalies on the ridge flanks (Cande and Kent, 1995) are consistent with the accretion of Penrose-type layered magmatic crust. Kardell et al. (2019) calculated ages and spreading rates from magnetic data acquired during the CREST cruise. Ages of the primary sites are estimated at 6.6, 15.2, 30.6, 49.2, and 61.2 Ma with half spreading rates of 17.0, 25.5, 24.0, 19.5, and 13.5 mm/y, respectively (Table **T1**). If 20 mm/y is used to separate slow and intermediate spreading rates (Perfit and Chadwick, 1998), then the primary sites were emplaced at both slow and intermediate spreading rates.

Seismic imaging along the CREST transect shows, at all ages from 0 to 65 Ma, an abundance of unsedimented, exposed basement outcrops that may allow the ingress and egress of seawater and ridge flank hydrothermal fluids. This suggests that the crust is never fully sealed by sediment at these ages (Estep et al., 2019) and that there may be long-lived and ongoing connection between the oceans and uppermost basaltic crust with implications for biogeochemical exchanges and subsurface microbial activity. All primary and alternate sites are positioned in localized sedimentary basins that are imaged on seismic reflection profiles. Unsedimented basement ridges are within 1–2 km of most primary sites (Figure **F4**). Sediment thicknesses were calculated using a constant sediment velocity of 1800 m/s.

## 4. Scientific objectives

The primary objective for Expedition 395E was to complete the work started during Expedition 390C, which was to lay the foundation for Expeditions 390 and 393 by coring a single hole to contact with hard rock and installing reentry systems at each site. By completing reentry system installations in advance, we better guarantee that the operational goals for Expeditions 390 and 393 can be achieved, particularly RCB coring ~250 m into basement at each site. For the APC/XCB hole at each Expedition 395E site, we intended to capture the sediment/basement interface using the XCB system with a polycrystalline diamond compact (PDC) cutting shoe and advance up to 5 m into hard rock material to (1) identify the depth of the contact with hard rock and (2) recover this critical boundary for future sampling and study. During Expedition 390C, this system provided good recovery of the upper basement with minimal disturbance, complimenting RCB coring planned for Expeditions 390 and 393. This interface is critical to documenting chemical exchange, alteration, and microbiological processes.

Specifically, the following were the precruise operations objectives for each Expedition 395E site:

- Proposed Site SATL-25A (~15.2 Ma crust): core with APC/XCB to 110 m and install reentry system to 109 mbsf. (This became Site U1560.)
- Proposed Site SATL-33B (~30.6 Ma crust): core with APC/XCB to 145 m and install reentry system to 144 mbsf. (This site was deferred to Expeditions 390 and 393 because of time constraints.)
- Site U1556 (~61.2 Ma crust): install reentry system to 284 mbsf. (This site was cored to 284 mbsf during Expedition 390C.)
- Site U1557 (~61.2 Ma crust): install casing to 570 mbsf to extend the reentry system that was installed to 60 m during Expedition 390C.

Because the APC/XCB cores collected during Expedition 395E will be treated as Expedition 390 and 393 samples, an additional objective of Expedition 395E was to measure ephemeral properties of the APC/XCB cores. These include *in situ* formation temperature measurements made with the advanced piston corer temperature (APCT-3) tool, physical properties, linescan images, X-ray images on the whole-round (WR) and split-core tracks, and paleomagnetic measurements on the archive halves. In addition, we collected one sample per core for headspace gas analysis as well as one to two WR samples per core for chemical analysis of interstitial water (IW). Geochemical data will guide chemical and microbiological sampling during Expeditions 390 and 393. A final objective was to collect samples to be distributed to micropaleontologists staffed during Expeditions 390 and 393 so that a preliminary biostratigraphic age model can be developed.

Expeditions 390 and 393 have three main scientific objectives.

## 4.1. Objective 1 (primary): quantify the timing, duration, and extent of ridge flank hydrothermal fluid-rock exchange

### 4.1.1. Scientific justification

Hydrothermal circulation at MORs and across their vast ridge flanks influences tectonic, magmatic, and microbial processes on a global scale; is a fundamental component of global biogeochemical cycles of key elements and isotopes (e.g., O, S, Mg, Fe, Li, B, Tl, and  $^{87}\text{Sr}$ ); and facilitates geological  $\text{CO}_2$  sequestration within the ocean crust. The chemical and isotopic composition of seawater reflects the dynamic balance between riverine inputs from the continents, burial of marine sediments, and hydrothermal exchanges with the ocean crust (e.g., Palmer and Edmond, 1989). Ocean crust is young and chemically homogeneous compared to continental crust, and its chemical exchanges with seawater are limited to a few relatively well-known reactions. Consequently, hydrothermal contributions to ocean chemistry are simpler to reconstruct than riverine inputs (Coggon and Teagle, 2011; Davis et al., 2003; Vance et al., 2009). Knowledge of the rates and magnitudes of hydrothermal exchanges will help us to decipher the changing global conditions responsible for past variations in seawater chemistry such as mountain building, changes in sea-floor spreading rate, large igneous province emplacement, changing climate, and evolution of biological systems. Building this knowledge requires ocean basin-wide transects across ridge flanks with different hydrogeologic histories.

Conductive heat flow deficits indicate that, on average, hydrothermal exchange persists at low temperatures ( $\ll 100^\circ\text{C}$ ) to 65 Ma on the ridge flanks (Stein and Stein, 1994). Given the vast extent of the ridge flanks, the hydrothermal fluid flux through them is many orders of magnitude greater than that through high-temperature ( $\le 400^\circ\text{C}$ ) axial systems (Mottl, 2003) and is likely important for elements for which fluid-rock exchange occurs at low temperatures (e.g., Mg, K, S, Li, B, C, and  $\text{H}_2\text{O}$ ). Hydrothermally altered ocean crust provides a time-integrated record of geochemical exchange with seawater manifested through changes in its chemical and isotopic composition, mineral assemblages, and physical properties (e.g., porosity, permeability, and seismic properties). The intensity of seawater-basalt exchange depends on the crustal age, architecture and thermal history, sediment cover, and spreading rate. Consequently, hydrothermal contributions to global geochemical cycles depend on the global length of slow-, intermediate-, and fast-spreading ridges and the age-area distribution of the ridge flanks, which varied significantly throughout the Phanerozoic (Müller et al., 2008). However, the impact of these variations on geochemical cycles is uncertain because the magnitude and spatial and temporal distribution of crust-seawater hydrothermal exchanges are poorly quantified. For example, the role of MOR spreading in controlling past atmospheric  $\text{CO}_2$  and hence climate remains controversial (Alt and Teagle, 1999; Berner et al., 1983; Gillis and Coogan, 2011; Staudigel et al., 1989) because of uncertainties regarding the rate, extent, and duration of hydrothermal  $\text{CaCO}_3$  precipitation due to our sparse sampling of intermediate age ocean crust (Figure F5). The hydrothermal carbonates that sequester  $\text{CO}_2$  in the ocean crust also record the composition of the fluids from which they precipitate (Coggon et al., 2004) and provide an exciting opportunity to develop medium-resolution records of past ocean chemistry (e.g., Mg/Ca and Sr/Ca) (Coggon and Teagle, 2011; Coggon et al., 2010; Rausch et al., 2013) that integrate past changes in major Earth system processes such as plate tectonics, mountain building, and climate. However, this approach is limited by sparse sampling of ocean crust of a variety of ages.

Drilling experiments on the Juan de Fuca Ridge flank were a key investigation of hydrothermal evolution across a ridge flank but were restricted to young ( $< 3.6$  Ma), intermediate-spreading (29 mm/y half spreading rate) crust (Shipboard Scientific Party, 1997; Expedition 301 Scientists, 2005; Expedition 327 Scientists, 2011). There is a dearth of holes in 20–120 Ma intact in situ MOR crust, and there are no significant penetrations ( $> 100$  m) of 46–120 Ma crust (Figure F5) (Expedition 335 Scientists, 2012). Consequently, the critical thermal, hydrogeologic, chemical, and microbial transitions across the ridge flanks remain unknown (Figure F2). Our current sampling of in situ upper ocean crust ( $> 100$  m) is biased toward areas with anomalously thick sediment for their crustal ages (Figure F3), and the majority of holes in ocean crust older than 35 Ma penetrate intermediate- or fast-spreading crust. The recovery of uppermost basement sections along the SAT across

slow/intermediate-spreading MAR crust will address these sampling gaps with respect to age, spreading rate, and sediment thickness.

Crustal accretion along the northern MAR is complex, and there are significant regions where spreading is accommodated by amagmatic extension by detachment faults that exhume sections of deep lithosphere to form OCCs (Mallows and Searle, 2012). However, a recent survey of the modern southern MAR during Cruise MSM25 of the R/V *Maria S. Merian* (2013) found no OCCs between 25°S and 33°S (Devey, 2014). This, combined with the relatively well defined marine magnetic anomalies on the southern MAR flanks (Maus et al., 2009), is consistent with accretion of intact magmatic crust. Because the ~31°S SAT follows a crustal flow line through a relatively long spreading segment (~100 km) away from major transform faults, we expect a Penrose-type stratigraphy of lavas overlying dikes and gabbros to have been accreted along the transect (Penrose Conference Participants, 1972).

#### 4.1.2. Expected outcomes

Hydrothermal alteration of basement cores will be investigated using a combination of petrological and geochemical analyses, radiometric dating, and detailed quantitative core logging of rock types, alteration features, and veins. The recovery of thinly sedimented slow/intermediate-spreading ocean crust along the proposed SAT will provide the following opportunities:

- To determine the nature, rates, magnitudes, distribution, and duration of hydrothermal alteration across the ridge flank;
- To investigate the effect of titanomagnetite/titanomaghemite alteration on the magnetic anomaly signal to elucidate its origin;
- To compare hydrothermal alteration of the uppermost slow/intermediate-spreading crust with crust of similar ages produced at faster spreading ridges (e.g., Holes 504B and 1256D);
- To evaluate the effect of changes in global spreading rates and the age-area distribution of the seafloor on hydrothermal contributions to global biogeochemical cycles; and
- To investigate signatures of changing ocean chemistry in the hydrothermal record and develop medium-resolution records of past ocean chemistry using hydrothermal minerals (following Coggon et al., 2010).

It will also allow us to test the following hypotheses:

- Hydrothermal chemical exchange ceases within 20 My of crustal formation.
- Basement topography and sedimentation history affect the rate and duration of hydrothermal alteration.

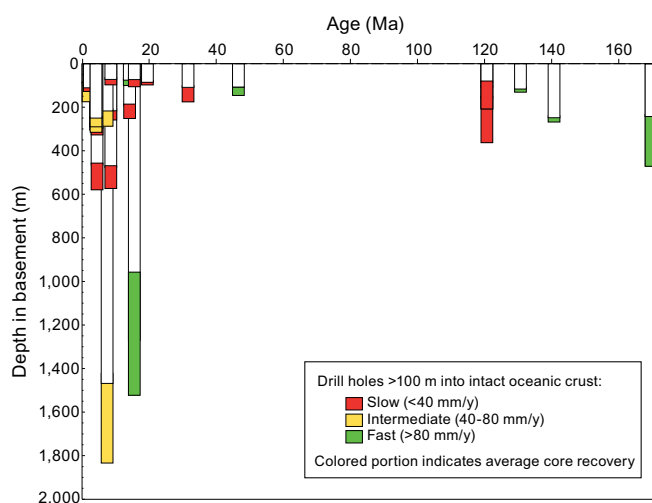


**Figure F5.** Compilation of all scientific ocean drilling holes that penetrate >100 m into intact upper (basaltic) ocean crust vs. crustal age. Spreading rates at which drilled sections formed are shown.

## 4.2. Objective 2 (primary): investigate sediment- and basement-hosted microbial community variation with substrate composition and age

### 4.2.1. Scientific justification

Scientific ocean drilling has revealed that microorganisms, Archaea, Bacteria, and eukaryotic fungi and protists are present, intact, and metabolically active in uncontaminated deep subsurface sediment and basalt. Knowledge about subseafloor microbial communities has grown exponentially since the initial microbial investigations by DSDP in the 1980s, but <4% of ODP/Integrated Ocean Drilling Program/IODP sites sampled have been sampled, documented, or archived for microbiological purposes (Kallmeyer et al., 2012; Orcutt et al., 2014). Determining microbial community composition and physiological capabilities along the SAT will provide insights into the role of microbes in mineral alteration, hydrocarbon formation, and global biogeochemical cycles.

In sediments, the number of microbial cells present is estimated to equal that in the entire oceanic water column (Kallmeyer et al., 2012). However, the amount of biomass stored in the deep subsurface remains contentious because microbial cell abundance in subseafloor sediment varies by approximately five orders of magnitude with significant geographic variation in the structure of subseafloor communities (Inagaki et al., 2006). The majority of studies have focused on relatively high biomass continental shelf systems (Inagaki and Orphan, 2014). Recent efforts, including Integrated Ocean Drilling Program Expeditions 329 (South Pacific Gyre; Expedition 329 Scientists, 2011) and 336 (North Pond; Expedition 336 Scientists, 2012), investigated lower biomass sedimentary systems underlying oceanic gyres. Crucially, no data have been collected from the South Atlantic Gyre (SAG). Such data would refine the global biomass census and improve our understanding of the global carbon cycle.

The presence or absence of oxygen in marine sediments has profound implications for the quantity, diversity, and function of microbial communities. Oxygen penetration depth varies between oceanic regions and settings, ranging from only a few millimeters in areas with high rates of microbial respiration, such as on continental shelves, to the entire sediment column in extremely low biomass sediments, such as those beneath the South Pacific Gyre (D'Hondt et al., 2015). Extrapolation of an observed global relationship between oxygen penetration and sedimentation rate and thickness indicates SAG sediment may be oxic to basement (D'Hondt et al., 2015). During Leg 3, oxygen was not measured, but sulfate was detected near the basement. However, sediment organic carbon concentrations along the SAT are intermediate to those of North Pond, where oxygen penetrated tens of meters below seafloor and nitrate was present to basement, and Nankai Trough, where oxygen was depleted by 3 mbsf and sulfate was depleted by 19 mbsf (Expedition 336 Scientists, 2012; Tobin et al., 2009; Orcutt et al., 2013; Reese et al., 2018). This indicates that oxygen is unlikely to extend to the basement at sites along the SAT, contrary to model predictions (D'Hondt et al., 2015), and that the classical redox succession of oxygen respiration followed by nitrate reduction, potentially followed by metal reduction, may be present. However, we hypothesize that oxygen will be reintroduced at the bottom of the sediment column as a result of oxygenated fluid flow in the uppermost volcanic basement, which is the case at North Pond (Expedition 336 Scientists, 2012). The recovery of the sediment package will allow us to address this conundrum regarding oxygen penetration, biomass, and carbon limitation of microbial activity.

We will compare the phylogenetic diversity, functional structure, and metabolic activity of SAG communities with results from previously studied regions. By exploiting the variations in sediment carbon composition expected across the subsiding MOR flank, we can examine the response of autotrophy versus heterotrophy to carbonate chemistry. Additionally, previous studies of the sedimentary deep biosphere have explored community diversity based on site-to-site or downhole (age) comparisons, often implicitly assuming a similar “starter community” that colonized the seafloor and whose structure and function subsequently changed in response to evolving geochemical conditions or burial depth. However, recent work suggests energy limitation may preclude replication (Lever et al., 2015; Lomstein et al., 2012) and thus limit community changes. The proposed age-transect approach will allow us to test this assumption directly by investigating the

impact of burial depth and chemical zonation on sediment of the same age and hence the same starter community.

Given the dearth of basement holes in ocean crust of intermediate age, there are no microbiological samples across the critical ridge–flank transitions in basement properties that may affect microbial communities (Figure F2). The majority of biological alteration of subseafloor basalts is thought to occur within 20 My of crustal formation (Bach and Edwards, 2003). However, microbiological investigations of oceanic basement have focused on young (<10 Ma) crust (Jungbluth et al., 2013; Lever et al., 2013; Mason et al., 2010; Orcutt et al., 2011) or older (>65 Ma) lava associated with hotspot volcanism along the Louisville seamount trail (Expedition 330 Scientists, 2012; Sylvan et al., 2015). Basement outcrops that penetrate the relatively impermeable sediment provide permeable conduits that facilitate subseafloor fluid circulation in older basement (Wheat and Fisher, 2008). Fluid flow across the sediment/basement interface can produce redox gradients that provide recharge of depleted electron acceptors (e.g., oxygen and nitrate) to basal sediments, as observed above 3.5 and 8 Ma ocean crust on the Juan de Fuca Ridge flank (Engelen et al., 2008) and at North Pond (Orcutt et al., 2013), respectively. However, the extent and duration of fluid flow through this interface across the ridge flanks remains unknown (Figure F2). The recovery of the uppermost basaltic basement from 7 to 61 Ma along the SAT will allow us to determine whether microbial populations are indeed present in basement older than 20 Ma and to investigate the nature, extent, and duration of communication between the sedimentary and crustal biosphere for the first time.

#### 4.2.2. Expected outcomes

We will sample subseafloor populations of Bacteria, Archaea, and microbial eukaryotes in both the sedimentary and upper crustal ecosystems along the proposed transect, quantify their biomass by cell enumeration, identify them using molecular biology methods, measure the stable isotopic composition (C, N, and S) of sediment and basement to relate processes to geochemistry, measure their metabolic activities using a variety of incubation assays, and resolve their physiological adaptations with omics-based approaches with the following aims:

- To evaluate cell abundance and community activity in the low energy subseafloor biosphere of the SAG and refine estimates of global subseafloor sedimentary microbial abundance;
- To resolve model predictions about the depth of oxygen penetration into sediment from overlying seawater and into the bottom of the sediment package from oxygenated fluid in basement;
- To evaluate the role of subseafloor microbes in sediment biogeochemistry and basement alteration and hence global biogeochemical cycles; and
- To investigate how aging of the ocean crust influences the composition of the crustal biosphere, particularly the effects of changing oxidation state and permeability on microbial abundance, diversity, and function.

Our samples will also allow us to test the following hypotheses:

- SAG microbial communities share membership and function with both oligotrophic sediments, like those found at North Pond, and open-ocean systems with higher organic matter input, such as the Nankai Trough, given the intermediate organic carbon content of the SAT sites.
- Microbial community structure and diversity depend on the starter community (and hence sediment age) rather than subsequent selection driven by burial or chemical zonation.
- Crustal biomass decreases with increasing basement age, and communication between the sedimentary and crustal biosphere ceases within 20 My.
- Microbial diversity increases within subseafloor basalts with basement age as previously demonstrated in basalts exposed on the seafloor (Lee et al., 2015; Santelli et al., 2009).

### 4.3. Objective 3 (secondary): investigate the responses of Atlantic Ocean circulation patterns and the Earth's climate system to rapid climate change including elevated atmospheric CO<sub>2</sub> during the Cenozoic

#### 4.3.1. Scientific justification

Climate change due to increased atmospheric CO<sub>2</sub> poses significant and imminent threats to global society and the environment. Knowledge of past ocean circulation patterns and temperatures is required to assess the efficacy of numerical models in simulating intervals of high *p*CO<sub>2</sub>. High *p*CO<sub>2</sub> intervals are often characterized by relatively shallow lysocline and calcite compensation depths (CCDs) resulting in poor preservation of CaCO<sub>3</sub> microfossils used to reconstruct paleoceanographic records. This problem can be overcome by coring sediment deposited on basement slightly older than the targeted sediment age that accumulated prior to thermal subsidence of the seafloor below the CCD. More continuous composite stratigraphic sequences are obtained by drilling multiple sites along a crustal age transect, a strategy successfully employed during ODP Leg 199 (Shipboard Scientific Party, 2002) and Integrated Ocean Drilling Program Expedition 320/321 (Pälike et al., 2012). The Walvis Ridge depth transect sampled during ODP Leg 208 demonstrated the dynamic nature of the Cenozoic CCD and lysocline in the southeastern Atlantic (Shipboard Scientific Party, 2004) and the value of redrilling previous transects to collect more complete records of Earth's history. Although spot cored, Leg 3 sites demonstrate moderate to excellent carbonate preservation along the SAT (Scientific Party, 1970) and the location's suitability for high-resolution paleoclimatic and paleoceanographic reconstructions through key intervals of rapid climate change (Cramer et al., 2009; Zachos et al., 2001, 2008), including the PETM and other short-lived hyperthermals, early and middle Eocene climatic optima, the onset of Antarctic glaciation across the Eocene/Oligocene boundary (O1 event), multiple Oligocene and Miocene glaciation events (O1 and Mi events), the Miocene climatic optimum and Monterey Carbon Excursion, Pliocene warmth, and the onset of Northern Hemisphere glaciation.

Global ocean circulation transfers heat and nutrients around the globe, both influencing and responding to changes in Earth's climate system (Broecker, 1991; Stommel, 1961; Wunsch, 2002). Fortunately, the western intensification of ocean currents means we can substantially reconstruct deepwater mass properties and thus thermohaline circulation history by characterizing western portions of major ocean basins using drilling transects. The western South Atlantic is the main northward flow path of Antarctic Bottom Water and southward flow path of North Atlantic Deep Water and their precursor water masses. Consequently, the SAT cores will provide complementary data needed to constrain the evolution of thermohaline circulation patterns and climate change as the Drake Passage and Southern Ocean opened, the northern North Atlantic deepwater gateway opened, and the Tethys Ocean became restricted to thermohaline circulation. In particular, these cores will assist in establishing how high-latitude sea surface (and hence deep ocean) temperatures and the CCD varied in response to *p*CO<sub>2</sub> changes and ocean acidification (Barker and Thomas, 2004; Barrera et al., 1997; Billups, 2002; Bohaty et al., 2009; Cramer et al., 2009; Frank and Arthur, 1999; Kennett and Stott, 1991; Scher and Martin, 2006; Thomas et al., 2003; Wright et al., 1991, 1992). The SAT will yield a complementary record to western North Atlantic sediments (Integrated Ocean Drilling Program Expedition 342; Norris et al., 2014), and together these data will provide an exceptional record of the evolution of Atlantic overturning circulation through the Cenozoic.

A novel, direct way to compare paleoceanographic reconstructions of past high *p*CO<sub>2</sub> to modern conditions is to recover sediments along transects of water column data collected by the World Ocean Circulation Experiment (WOCE). The SAT constitutes a "paleo-WOCE" line following the western portion of WOCE Line A10 (Figure F1), providing access to paleoceanographic records of southern and northern-sourced deep and bottom waters. We will test models of bipolar deepwater evolution (e.g., Borrelli et al., 2014; Cramer et al., 2009; Katz et al., 2011; Tripati et al., 2005) using stable and radiogenic isotope analyses of sediments recovered from these key western South Atlantic sites.

The Walvis Ridge depth transect (Shipboard Scientific Party, 2004) revealed a dramatic 2 km CCD shoaling during the PETM due to the acidification of the ocean from massive carbon addition fol-

lowed by a gradual recovery (Zachos et al., 2005; Zeebe et al., 2008). Given chemical weathering feedbacks, the recovery of the CCD should have resulted in a transient overdeepening of the CCD (Dickens et al., 1997). Collectively, the SAT sites will provide additional data for reconstructing changes in the position of the lysocline and CCD in the western South Atlantic that are essential for constraining the timing of gateway events and the history of Northern Component Water and Southern Component Water, which were the precursors to North Atlantic Deep Water and Antarctic Bottom Water, and the nature of Atlantic basin responses to climate change relative to the Pacific.

#### 4.3.2. Expected outcomes

Microfossils provide a critical archive of ocean and climate history, including long-term changes (e.g., early Eocene warmth, Cenozoic cooling, and Pliocene warmth) and abrupt events (e.g., early Paleogene hyperthermals and multiple glaciation events). Complete sedimentary sections recovered along paleo-WOCE Line A10 will exploit thermal subsidence of the ocean crust along the transect to provide material for high-resolution proxy records including benthic and planktonic foraminiferal geochemistry, micropaleontological assemblages, orbitally tuned age models, neodymium isotopes, and alkenone  $\delta^{13}\text{C}$  and boron isotope  $p\text{CO}_2$  reconstructions with the following aims:

- To reconstruct the evolution of deepwater masses over the past 61 My to assess contributions of Northern Component Water and Southern Component Water in the early Paleogene western South Atlantic (Kennett and Stott, 1990) and to document the influence of the openings of the Drake and Tasman Passages on South Atlantic deepwater circulation;
- To provide high-resolution constraints on CCD and carbonate chemistry changes of the deep western Atlantic, particularly during transient hyperthermals and other intervals of global warmth;
- To reconstruct the Cenozoic history of the South Atlantic subtropical gyre by monitoring proxies of productivity and paleobiogeography of oceanic plankton, rates of speciation/extinction relative to those of the equatorial zone and higher latitudes, and changes in biodiversity and subtropical ecosystem dynamics; and
- To evaluate the response of subtropical planktonic and benthic biota to changing environmental conditions such as global warming, ocean acidification, or fertility patterns during intervals of rapid climate change through the Cenozoic.

Drilling at these sites will also allow us to test the following hypotheses:

- Low-latitude sites were potential sources of deepwater formation at times of global warmth and high atmospheric  $p\text{CO}_2$ .
- The strength of the coupling between the climate and the carbon cycle varied through the Cenozoic.
- The lysocline and CCD responded differently on the western side of the MAR compared to the Walvis Ridge record due to changing deep/bottom water sources, gateway configurations, and flow paths.
- The subtropical gyre cut off the delivery of heat to Antarctica as the Antarctic Circumpolar Current developed through the late Eocene–Oligocene.

### 5. Site summaries

#### 5.1. Beginning of expedition and transit

Expedition 395E (Complete South Atlantic Transect Reentry Systems) started in Cape Town, South Africa, at 0800 h (UTC + 2 h) on 6 April 2021. There was no science party on the ship during Expedition 395E because of COVID pandemic travel restrictions and safety concerns. JRSO personnel had arrived in Cape Town on 1 April to quarantine in the hotel for 7 days prior to boarding. They took COVID-19 tests on 4 and 7 April, and these tests returned negative results, enabling the JRSO personnel to board the R/V *JOIDES Resolution* on 8 April.

However, three of the Siem Offshore crew tested positive for COVID-19 in the hotel, so they and their 14 close contacts quarantined longer than originally planned. The extra quarantine time meant that the ship was not able to depart as originally scheduled on 11 April. These crew members were tested again on 11 April and the results came back negative for the close contacts. On 13 April, an additional round of testing of all shipboard personnel was conducted dockside, with everybody testing negative. The 14 close-contact crew members boarded *JOIDES Resolution* early on 15 April. The three original cases were not allowed to join the ship and returned home at the earliest opportunity.

During the port call, the fiber-optic pigtail on the vibration isolated television subsea camera was upgraded by a contractor (a former IODP staff member), and the job was completed by 11 April.

The harbor pilot boarded the vessel at 0922 h on 15 April, and the last dock line was released at 1000 h. The pilot was away at 1026 h and the sea voyage started at 1100 h (Figures F6, F7). Shipboard personnel wore masks and followed social distancing protocols during the 14 day COVID-

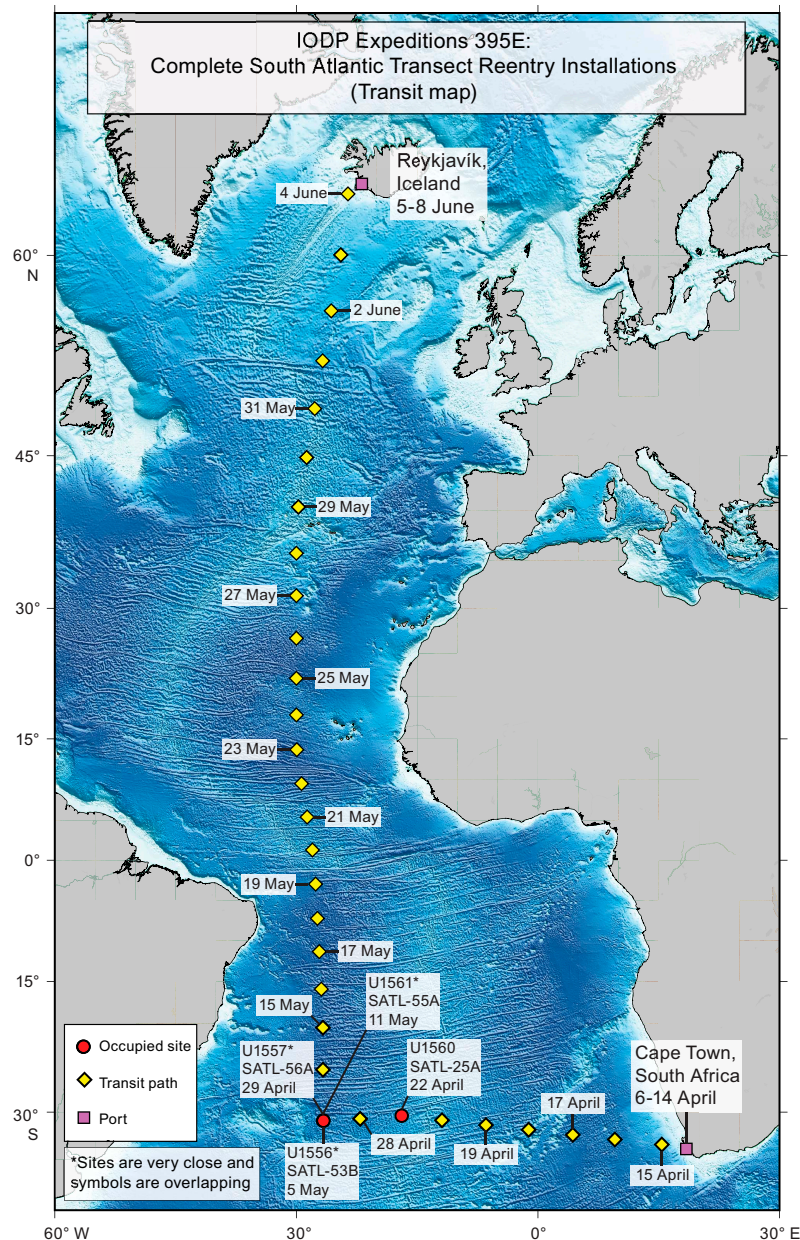


**Figure F6.** Transit and site location map, Expedition 395E.

19 mitigation period following the departure of the pilot. During the transit, the ship's clock was set back 2 h, putting the ship at UTC + 0, or 5 h ahead of College Station, Texas. The ship stayed on that time until the end of the expedition in Reykjavík, Iceland.

We arrived at Site U1560 at 0108 h on 22 April, completing the 1817 nmi transit from Cape Town in 161.3 h (6.7 days) at an average speed of 11.3 kt. The thrusters were lowered, and the ship switched to dynamic positioning (DP) mode at 0215 h, starting operations for Site U1560.

## 5.2. Site U1560

### 5.2.1. Background and objectives

Site U1560 (Proposed Site SATL-25A) is at 30.4°S in the central South Atlantic Ocean, ~315 km west of the MAR. The objective for Site U1560 during Expedition 395E was (1) to core one hole with the APC/XCB system to basement for gas safety monitoring and to confirm the depth to basement and (2) to install a reentry system with casing through the sediment into basement in a second hole (Figure F8). These operations will expedite basement drilling during SAT Expeditions 390 and 393.

Site U1560 is located on Seismic Line CREST02 at common depth point (CDP) 12770, ~400 m south of the CREST1E crossing line. A reflector at ~5.08 s two-way traveltimes (TWT) was interpreted to be the top of basement and estimated to be 104 mbsf (Coggon et al., 2020). Based on the deeper-than-expected basement depths we found during Expedition 390C, we expected basement to be similarly deeper at Site U1560. The ocean crust at Site U1560 was estimated to have formed at 15.2 Ma at a half spreading rate of 25.5 mm/y. This site targets the second-youngest crust of the SAT sites. The mineralogy and alteration extent of the basement rocks at Site U1560, changes in physical properties such as porosity, and the composition of the microbial communities will be compared to the same characteristics at the other sites along the transect to investigate the development of hydrothermal circulation and crustal aging. Overlying sediment at Site U1560 is primarily carbonate ooze and will be used in paleoceanographic and microbiological studies.

	Sunday	Monday	Tuesday	Wednesday	Thursday	Friday	Saturday
	18	19	20	21	22	23	24
April	Transit	Transit	Transit	Transit	Site U1560 (SATL-25A) coring	Site U1560 (SATL-25A) coring	Site U1560 (SATL-25A) coring
	25	26	27	28	29	30	1
	Site U1560 (SATL-25A) reentry	Site U1560 (SATL-25A) reentry	Site U1560 (SATL-25A) reentry	Transit	Transit	Site U1557 (SATL-56A) reentry	Site U1557 (SATL-56A) reentry
	2	3	4	5	6	7	8
	Site U1557 (SATL-56A) reentry	Site U1557 (SATL-56A) reentry	Site U1557 (SATL-56A) reentry	Site U1556 (SATL-53B) reentry			
	9	10	11	12	13	14	15
May	Site U1556	WOW	Site U1561 (SATL-55A) coring	Site U1561 (SATL-55A) coring	Site U1561 (SATL-55A)	Transit	Transit
	WOW	Site U1556 reentry			Transit		
	16	17	18	19	20	21	22
	Transit						

**Figure F7.** Operations schedule, Expedition 395E. *JOIDES Resolution* departed Cape Town, South Africa, on 15 April 2021 and arrived in Reykjavík, Iceland, on 5 June. WOW = waiting on weather.

## 5.2.2. Operations

### 5.2.2.1. Hole U1560A

*JOIDES Resolution* completed the 1817 nmi transit to Site U1560 from Cape Town in 6.7 days at an average speed of 11.3 kt. We arrived at Site U1560 at 0108 h on 22 April 2021 (Figures F6, F7), lowered the thrusters, and switched to DP mode at 0215 h, marking the start of operations at Site U1560. The APC/XCB bottom-hole assembly (BHA) was made up, and we started lowering the drill bit to the seafloor at 0945 h. During the descent, the brakes on the drawworks unit were found to be slipping, and tripping was paused several times for adjustments. The drill string deployment was stopped at 1900 h to inspect the brakes. Everything appeared normal, except the bands appeared to be dusty. The bands were washed off and the covers reinstalled. The brakes operated normally after this. Tripping resumed at 2250 h to 3708 meters below sea level (mbsl). Because this was the first site of the expedition, we pumped two “pigs” (pipe cleaning devices) through the drill string to remove rust. The first APC core was shot from 3714 mbsl but returned empty, missing the mudline, so the drill bit was lowered 5 m for the next attempt.

We spudded Hole U1560A ( $30^{\circ}24.2064'\text{S}$ ,  $16^{\circ}55.3718'\text{W}$ ) at 0405 h on 23 April. Mudline Core 395E-U1560A-1H arrived on deck at 0430 h and recovered 4.7 m (Figure F9), establishing a seafloor depth of 3723.7 mbsl. Cores 2H–11H advanced from 4.6 to 99.7 mbsf. All APC cores were oriented with the Icefield MI-5 core orientation tool. Formation temperature measurements were taken on Cores 4H and 7H with the APCT-3 tool.

At 1730 h, we changed to the XCB coring system because we were approaching the anticipated basement depth. We used a PDC XCB cutting shoe that had proven successful at recovering basement material during Expedition 390C. Cores 395E-U1560A-12X through 14X advanced from 99.7 to 120.1 mbsf. While drilling Core 15X, a slowing in the drilling rate indicated that the basement contact was reached at 120.2 mbsf (Figure F9). Cores 15X and 16X advanced from 120.1 to 122.5 mbsf and recovered 0.44 m (18%). Upon recovery, these two cores were confirmed to be basalt (Figure F10). The rate of penetration in this solid formation was slow (~0.6 m/h), so we stopped coring at this point. We raised the drill bit up to the ship, and it cleared the rig floor at 1520 h on 24 April, ending Hole U1560A. Cores 1H–16X recovered 119.08 m (97%). Total depth for Hole U1560A was 122.5 mbsf, and total time on hole was 61.05 h (2.5 days).

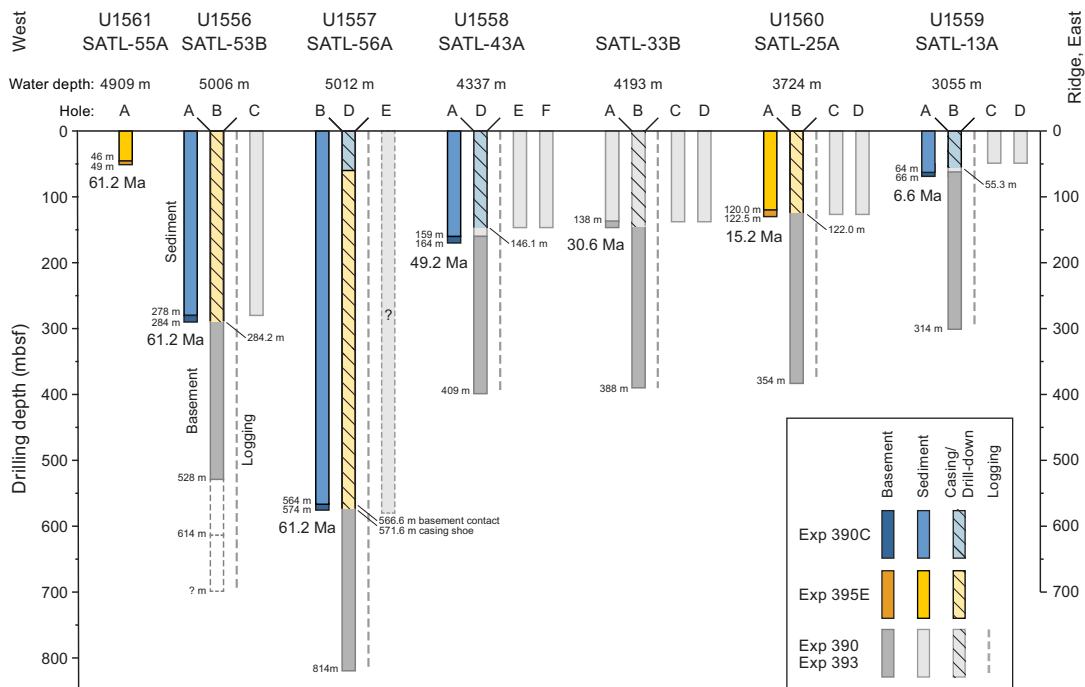


**Figure F8.** South Atlantic Transect operations completed during Expeditions 390C and 395E and remaining work to be done during Expeditions 390 and 393.

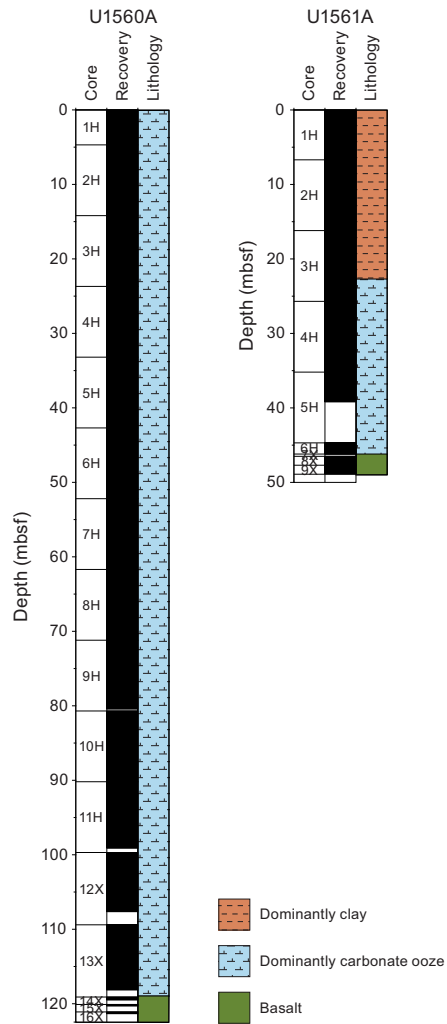


**Figure F9.** Core recovery and lithology, Holes U1560A and U1561A. Black = recovered core, white = no recovery.



**Figure F10.** Basalt, Holes U1560A and U1561A.

### 5.2.2.2. Hole U1560B

We then prepared to install the reentry system in Hole U1560B (Figure F11). At 1745 h on 24 April 2021, we started making up the HRT BHA, followed by the 10 $\frac{3}{4}$  inch casing string. We picked up the casing with the running tool and landed it on the base of the reentry cone in the moonpool. We then rigged up the drill pipe stinger, including a drill bit, underreamer, and mud motor, and tested it in the moonpool. By 1300 h on 25 April, we had lowered the stinger through the casing and secured it to the base. We assembled the reentry cone and welded it to the base, and at 1545 h we started lowering the assembly to the seafloor, reaching 3675 mbsl at 0130 h on 26 April. We installed the top drive and deployed the subsea camera and Conductivity-Temperature-Depth (CTD) instrument.

We spudded Hole U1560B ( $30^{\circ}56.4546'S$ ,  $26^{\circ}37.7898'W$ ) at 0430 h on 26 April. A water depth of 3723.7 mbsl was assumed, based on the mudline depth for Hole U1560A. In the subsea camera images, Hole U1560B lies about 5 m to the west-southwest of Hole U1560A. We drilled to the target depth of 124 mbsf and disconnected the casing using the HRT at 1025 h. We filled the cased hole with heavy mud to prevent inflow and raised the subsea camera and CTD instrument to the ship. We then raised the stinger assembly to the ship, and the drill bit reached the rig floor at 2355 h and was disassembled. Wear on the bit indicated that basement was contacted, but the excellent condition of the underreamer cutters suggests that it is unlikely that the underreamer and casing reached basement. Therefore, the basement contact in Hole U1560B is a little deeper than in Hole U1560A (120.2 mbsf), as a result of local basement surface topography.

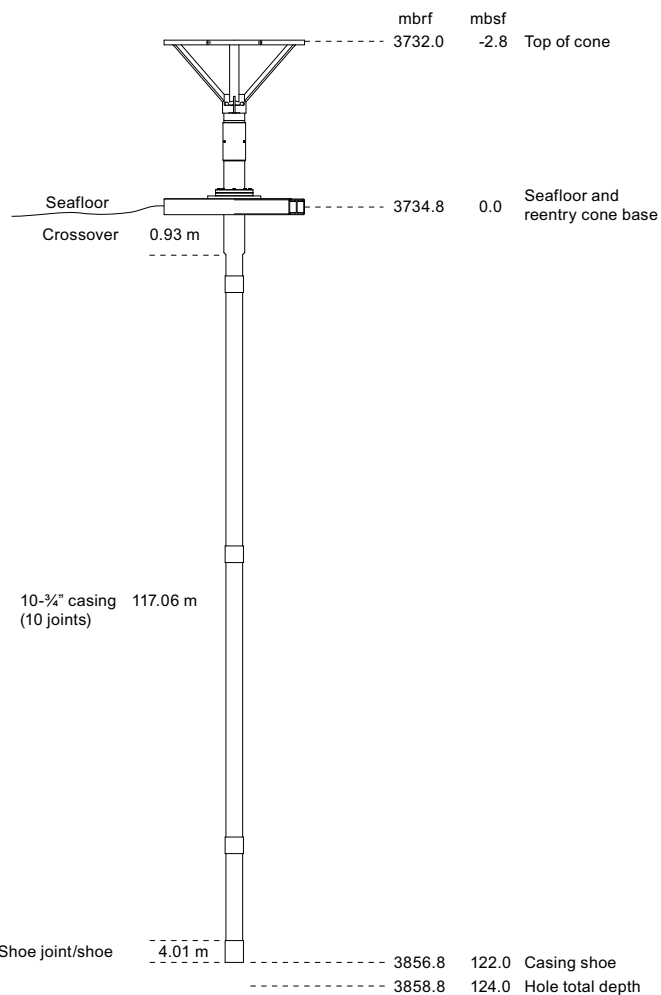


**Figure F11.** Reentry system, Hole U1560B. mbrf = meters below rig floor, mbsf = meters below seafloor.

We made up the cementing BHA and lowered it to just above the seabed. The subsea camera was lowered to the BHA to guide reentry, and at 1445 h on 27 April we reentered Hole U1560B. We positioned the base of the BHA at 3 mbsf, which was deep enough for the cup packer in the BHA to seal the top of the casing. We established circulation and pumped down 10 bbl of 15 ppg cement and then pulled the BHA back out of the hole, clearing the reentry cone at 1545 h. The drill pipe was cleared of any residual cement by pumping down two pigs and flushing it with seawater. The subsea camera was raised back to the ship, followed by the BHA, ending operations in Hole U1560B at 2315 h on 27 April. The rig floor was secured for transit at 0045 h on 28 April. We raised the thrusters and started the sea passage to Site U1557 at 0124 h on 28 April, ending operations at Site U1560.

The next site of Expedition 395E was originally planned to be Proposed Site SATL-33B, the middle site of the SAT on 30.6 Ma crust. Because of the 4 day delay in leaving port, there would not have been enough time to complete operations at all four planned sites, so we decided to defer operations at Site SATL-33B until Expedition 390 or 393 in 2022. Instead, the next hole of Expedition 395E was the higher priority Hole U1557D, where Expedition 390C had installed a reentry system consisting of a reentry cone and 60 m of 16 inch casing in November 2020. This site was technically more challenging because the heavy weight of ~5 km of pipe and 573 m of casing meant that the installation could only take place under calm conditions. The weather forecast predicted calm seas at Site U1557, and we decided to take advantage of that.

### 5.2.3. Principal results

The sediment/basement contact in Hole U1560A is a sharp transition at 120.1 mbsf. The contact was deeper than originally estimated from seismic data (104 mbsf) but similar to what was expected from the basement depths cored during Expedition 390C. The basement depth in cased Hole U1560B is slightly deeper than in Hole U1560A, but the exact depth in Hole U1560B remains to be determined by drilling and logging during Expedition 390 or 393.

Cores 395E-U1560A-1H through 14X were measured on the WR and split-core track systems. Cores 15X and 16X were measured on the WR tracks but were not split and were preserved in nitrogen gas-flushed bags for description and analysis during Expeditions 390 and 393. Core catcher samples from Cores 1H through 13X were collected for postexpedition biostratigraphic dating. In addition, we collected one sample per core for headspace gas analysis as well as 1 or 2 WR samples per core for chemical analysis of IW. The squeezed sediments from the IW samples were measured on the carbonate coulometer and X-ray diffraction (XRD) instruments. No systematic core description took place during Expedition 395E.

The sediment is predominantly carbonate ooze (Figure F9) that ranges from 81 to 95 wt% calcium carbonate. Generally low values of magnetic susceptibility and natural gamma radiation (NGR) reflect the low terrigenous content of the carbonate ooze, and 10 m to submeter-scale variations in these physical property values likely reflect variations in terrigenous sediment content. Paleomagnetic reversals are evident in the superconducting rock magnetometer (SRM) data, and a preliminary assessment of the reversal stratigraphy suggests that sedimentation is most probably continuous at this site since the crust formed ~15 Ma. It is likely that a robust magnetostratigraphy can be constructed after further holes are cored during Expedition 390 or 393 and a complete splice is available.

Preliminary analysis of the IW chemistry data shows that sulfate has a flat profile, varying between 27.4 and 28.8 mM. Ammonium has more variability, ranging from 3  $\mu$ M near the top of the hole to 40  $\mu$ M near its base. Most dissolved element profiles have some downhole structure but over narrow concentration ranges; for example, magnesium varies between 49.7 and 52.5 mM. Headspace methane measurements were all below the detection limit. These results suggest that diagenetic processes at Site U1560 are slow, which is consistent with this site's open-ocean location and low organic matter input.

## 5.3. Site U1557

### 5.3.1. Background and objectives

Site U1557 (proposed Site SATL-56A) was started during SAT Expedition 390C in November 2020. Site U1557 was cored to basement in Hole U1557B, and a reentry system consisting of a reentry cone and 60 m of 16 inch casing was installed in Hole U1557D (Estes et al., 2021). The objective for Expedition 395E was to complete the reentry system in Hole U1557D by installing a second, nested 10% inch casing string down to basement. This engineering work will expedite basement drilling during SAT Expeditions 390 and 393.

Site U1557 is in the central South Atlantic Ocean at 31°S at a water depth of 5010.7 m, ~1250 km west of the MAR. It lies on Seismic Line CREST1A/B at CDP 4470 near the CREST05 crossing line (Figure F4) (Coggon et al., 2020). A reflector at ~7.2 s TWT was interpreted to be the top of basement, and the sediment–basement transition was found at 564 mbsf in Hole U1557B. This site is located 6.7 km from Site U1556, and the ocean crust at both sites is estimated to have formed at ~61.2 Ma at a half spreading rate of ~13.5 mm/y. Ocean crust at these sites is the oldest that will be drilled along the SAT and will be compared to younger crustal material from the sites to the east, closer to the MAR. The sedimentary succession at Site U1557 is about twice as thick as at Site U1556. Contrasts between these closely spaced sites will allow exploration of the blanketing effect of sediment thickness on hydrothermal circulation and crustal evolution. The sediments at Site U1557 consist of calcareous ooze and hemipelagic clays and will be used in paleoceanographic and microbiological studies. The thick succession at Site U1557 will allow development of paleoceanographic records covering the entire Cenozoic, including reconstruction of Atlantic Ocean circulation patterns during periods of elevated atmospheric carbon dioxide.

### 5.3.2. Operations

#### 5.3.2.1. Hole U1557D

The ship transited 502 nmi from Site U1560 to Site U1557 in 44 h at an average speed of 11.4 kt, arriving at Hole U1557D (30°56.4546'S, 26°37.7898'W) at 2130 h on 29 April 2021 (Figures F6, F7). The thrusters were lowered, and the ship switched to DP mode at 2215 h. The plan was to first deepen Hole U1557D from the depth of the existing 16 inch casing shoe (60 mbsf) to 10 m into basement in preparation for installing the 10% inch casing string using a Dril-Quip running tool in a separate run (Figure F12). We used this two-stage method because the water depth (5010.7 mbsl) and casing depth (~573 mbsf) at Site U1557 meant that a mud motor stinger and HRT assembly, used in Hole U1560B, would be too heavy to deploy safely.

The 14½ inch drilling BHA was assembled at 0230 h on 30 April, and we ran it down to 4980 mbsl by 1100 h. We then deployed the subsea camera and CTD instrument. The camera worked well, confirming that the upgrade to the fiber-optic pigtail connection that had been made during the port call was successful (the connection had failed in these water depths during Expedition 390C). We picked up the top drive and reentered Hole U1557D at 1600 h, retrieved the subsea camera and CTD instrument, and brought them back on board at 1815 h. At 1830 h, we started lowering the BHA into the cased part of the existing hole, taking weight at 60 mbsf at 1930 h. Over the next 37 h we drilled down, and we reached the sediment/basement contact at 566.6 mbsf at 0830 h on 2 May. This compares to a basement depth of 564 mbsf in Hole U1557B. It took another 7.5 h to reach the target depth of 576.6 mbsf (Figure F8). We then swept the hole of cuttings by pumping 50 bbl of high-viscosity mud. Next, we made a wiper trip to clear the hole of obstructions and infill. We racked back the top drive and raised the drill bit to the base of the 16 inch casing (60 mbsf), and then lowered the drill bit back down to 524.1 mbsf. At that point, we reinstalled the top drive and rotated the drill bit down, encountered infill at 568.1 mbsf, and then washed it out to the total hole depth of 576.6 mbsf. We made another sweep of the hole with 50 bbl of high-viscosity mud, and then filled the hole with 12 ppg heavy mud to help reduce any caving of the borehole walls. On 3 May, we pulled the drill bit out of the hole, clearing the seafloor at 0315 h and reaching the rig floor at 1430 h. We assembled the casing running tool and set it aside in the derrick and then assembled the casing string, which took the remainder of the day. On 4 May, we lowered the casing string to 4978 mbsl, and at 1000 h we started to lower the subsea camera. We reentered Hole U1557D at 1245 h and lowered the casing string to 554 mbsf. At that depth, we engaged the top

drive to allow rotation, if required, and continued lowering the casing to its full depth of 571.6 mbsf at 1535 h, landing the top of the casing in the existing reentry cone. There was no circulation in the hole while pumping, showing that the formation had sealed around the casing and that the base of the casing would not need to be cemented. We released the casing from the Dril-Quip running tool and cleared the reentry cone at 1600 h.

Starting at 1645 h on 4 May, *JOIDES Resolution* moved from Hole U1557D to Site U1556 in DP mode, traveling 3.6 nmi in 12.5 h at an average speed of 0.3 kt. During this slow transit, the subsea camera was brought back aboard at 1830 h. We raised the BHA and the Dril-Quip casing running tool and then disassembled it by 0630 h on 5 May, officially ending operations in Hole U1557D. We arrived at Site U1556 at 0715 h on 5 May.

### 5.3.3. Principal results

The sediment/basement contact in Hole U1557D is at 566.6 mbsf, based on the abrupt reduction in drilling rate at that depth. This is 2.6 m deeper than the basement depth of 564 mbsf in Hole U1557B. The difference can be attributed to normal local variations in basement surface topography.

No material was cored in Hole U1557D during Expedition 395E. A basic description of the cores from Hole U1557B, cored during Expedition 390C, is available in the *Expedition 390C Preliminary Report* (Estes et al., 2021).

Additional analyses and data interpretations will occur during Expeditions 390 and 393, which are scheduled to take place in 2022.

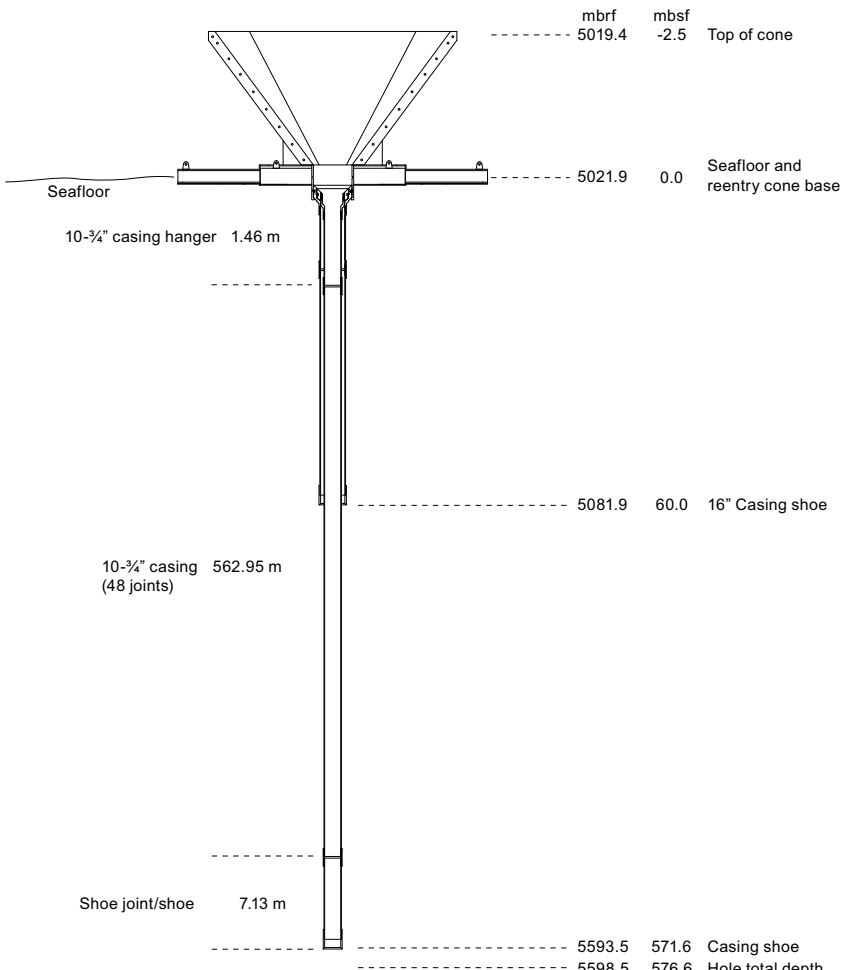


**Figure F12.** Reentry system, Hole U1557D. mbrf = meters below rig floor, mbsf = meters below seafloor.

## 5.4. Site U1556

### 5.4.1. Background and objectives

Site U1556 (proposed Site SATL-53B) started during SAT Expedition 390C in October 2020, when Hole U1556A was cored to basement (Estes et al., 2021). The objective for Expedition 395E was to drill and install a 10½ inch reentry system with casing to basement in Hole U1556B. These operations will expedite basement drilling during SAT Expeditions 390 and 393.

Site U1556 is in the central South Atlantic Ocean at 30.6°S at a water depth of 5006 m, ~1250 km west of the MAR. It lies on Seismic Line CREST1A/B at CDP 3410 near the CREST05 crossing line (Figure F4) (Coggon et al., 2020). A reflector at ~6.9 s TWT was interpreted to be the top of basement and was found at 278 mbsf in Hole U1556A. This site is located 6.7 km west of Site U1557, and the basement at both sites is predicted to have formed at ~61.2 Ma at a half spreading rate of ~13.5 mm/y. Oceanic crust at these sites is the oldest that will be drilled during the SAT expeditions. The mineralogy and extent of alteration of the basement rocks at Site U1556, changes in physical properties such as porosity, and the composition of the microbial communities will be compared to the same characteristics at the other sites along the transect to investigate the development of hydrothermal circulation and crustal aging. The sedimentary succession at Site U1556 is about half as thick as at Site U1557, and contrasts between these closely spaced sites will allow exploration of the blanketing effect of sediment thickness on hydrothermal circulation. Sediment in Hole U1556A alternates between 1–10 m thick layers of red-brown clay and carbonate ooze with sharp contacts between these lithologies (Estes et al., 2021) and will be used in paleoceanographic and microbiological studies.

### 5.4.2. Operations

#### 5.4.2.1. Hole U1556B

We arrived at Site U1556 at 0715 h on 5 May 2021 after moving from Site U1557 in DP mode (Figures F6, F7). In preparation for installing the reentry system in Hole U1556B (Figure F13), we made up the HRT and set it aside in the derrick. We then assembled 284.2 m of 10½ inch casing and landed it on the base of the reentry cone in the moonpool. From 1700 to 2215 h, we assembled the stinger (comprising a 9½ inch bit, underreamer, and mud motor), tested it in the moonpool, and lowered it down through the casing. The same assembly had been used to drill Hole U1560B earlier during the expedition. The HRT running tool was attached and bolted to the base of the reentry cone, and the reentry cone was welded to the base. At 0230 h on 6 May, we lowered the assembly through the moonpool and started the pipe trip to 4994 mbsl. At 1300 h, we started to lower the subsea camera.

We started Hole U1556B (30°56.5244'S, 26°41.9472'W) at 1655 h on 6 May, and by 2000 h we had drilled in the casing to 75.5 mbsf. During this operation, the cable to the subsea camera had wrapped around the drill pipe eight times, which is more than usual, so we paused drilling and slowly raised the subsea camera to the ship. It was back on board at 2245 h. We resumed drilling, and at 1530 h on 7 May at an apparent depth of 282.3 mbsf, the weight of the casing was no longer held by the drill string, indicating that the reentry cone had landed on the seafloor at a shallower depth than the expected 286.2 mbsf. At 1630 h, we released the casing from the HRT. We filled the hole with 75 bbl of heavy mud and raised the drill bit, clearing the seafloor at 1920 h. From 0245 to 1200 h on 8 May, we disassembled the bit, underreamer, and mud motor and then assembled the BHA for cementing.

After stowing the casing deployment equipment, we lowered the cementing BHA to 4922 mbsl. The next operation was to deploy the subsea camera to guide reentry into Hole U1556B. However, rough weather with ~4 m heave made it unsafe to launch the camera (at a water depth of 5000 m the camera's umbilical cable has a fatigue operating limit of ~2.5 m of heave), so we waited for the seas to subside. At 0945 h on 10 May, the seas had calmed enough to deploy the subsea camera. We observed that the top of the reentry cone was level with the seafloor (Figure F13) and tagged it to determine a water depth of 5001.8 mbsl for Hole U1556B. This depth is 4.6 m shallower than the mudline depth for Hole U1556A, which explains why the casing in Hole U1556B landed at a shal-

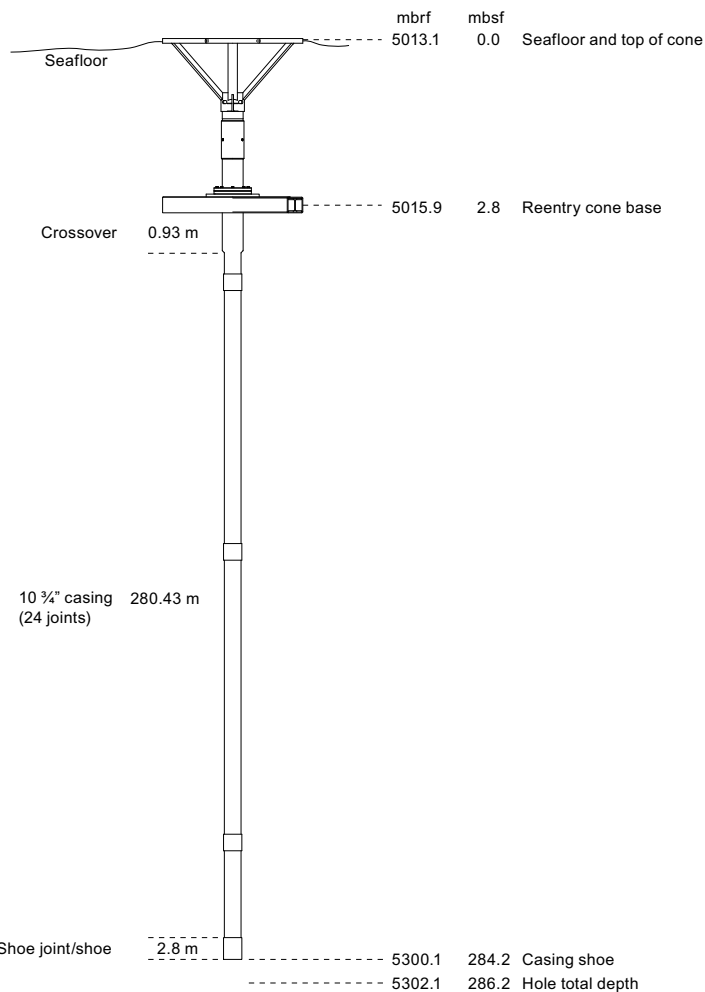


**Figure F13.** Reentry system, Hole U1556B. mbrf = meters below rig floor, mbsf = meters below seafloor.

lower depth than expected. Based on the water depth, the depth of Hole U1556B was revised to 286.2 mbsf, with the 10 3/4 inch casing shoe at 284.2 mbsf. As a result of the shallower-than-expected seafloor, Hole U1556B came close to but did not reach the sediment/basement contact.

At 1225 h on 10 May we reentered Hole U1556B with the cementing BHA. A circulation test showed that the formation had sealed around the casing, so there was no need to cement the base of the hole. We raised the BHA, which cleared the seafloor at 1240 h and reached the rig floor at 2359 h, ending operations in Hole U1556B.

#### 5.4.3. Principal results

Expedition 395E did not retrieve core material from Hole U1556B, but a description of the principal results from Hole U1556A, cored during Expedition 390C, are described in the *Expedition 390C Preliminary Report* (Estes et al., 2021). Additional analyses and data interpretation will take place during Expeditions 390 and 393, which are scheduled to take place in 2022.

### 5.5. Site U1561

#### 5.5.1. Background and objectives

Site U1561 (proposed Site SATL-55A) is in the central South Atlantic Ocean at 30.4°S, ~1250 km west of the MAR. It lies on Seismic Line CREST05 at CDP 16750 (Figures F1, F4). A reflector at ~6.56 s TWT was interpreted to be the top of basement at 126 mbsf (Coggon et al., 2020). This site is located 13 nmi north of Site U1556, and the basement at both sites is predicted to have formed

at ~61.2 Ma at a half spreading rate of ~13.5 mm/y. Oceanic crust at these sites is the oldest that will be drilled during SAT Expeditions 390 and 393.

After completing reentry system installations in Holes U1560B, U1557D, and U1556B for the SAT, ~2.5 days of operations time remained during Expedition 395E before we had to depart for Reykjavík on 14 May. In consultation with the Expedition 390/393 Co-Chief Scientists, it was decided to use this time to core a single hole at nearby alternate Site SATL-55A (U1561). The sedimentary succession at Site U1561 was expected to be thinner than at nearby Sites U1556 and U1557 and would provide information on sediment accumulation patterns and pore water chemical profiles of this local area.

### 5.5.2. Operations

#### 5.5.2.1. Hole U1561A

After completing the 13 nmi transit from Site U1556, we arrived at Site U1561 at 0324 h on 11 May 2021 (Figures F6, F7). We lowered the thrusters and entered DP mode at 0349 h. The APC/XCB BHA was made up and lowered to the seafloor. Based on the seafloor reflection in the seismic profile, the water depth at Site U1561 was expected to be 4857 mbsl (Coggon et al., 2020). As we arrived on site, the precision depth recorder (PDR) 3.5 kHz signal malfunctioned and the depth reading had to be taken with the 12.5 kHz signal instead, which gave an apparent water depth of 4963 mbsl (106 m deeper than the depth in the *Scientific Prospectus* [Coggon et al., 2020]). Because of this discrepancy, below 4857 mbsl we slowed the descent of the drill bit and monitored the weight of the drill string. The drill string took noticeable weight at 4927 mbsl, indicating that the BHA was partly supported by the formation. We raised the drill bit to 4917 mbsl to attempt a mudline core, which returned full, showing that the seafloor was shallower than 4917 mbsl. We raised the drill bit by a further 5 m to 4912 mbsl for a second attempt, but this core was also full and did not recover a mudline. These two cores were later designated to be Cores 395E-U1561B-1H and 395E-U1561C-1H, respectively. The drill bit was raised to 4907 mbsl for a third attempt.

Hole U1561A (30°43.2902'S, 026°41.7162'W) was spudded at 2335 h on 11 May, and Core 395E-U1561A-1H recovered 6.7 m, establishing a seafloor depth of 4909.5 mbsl. On 12 May, Cores 2H–6H advanced from 6.7 to 46.2 mbsf (Figures F8, F9). Core 6H struck hard rock, which bent the APC cutting shoe. We switched to the XCB system, and Cores 7X–9X advanced from 46.2 to 48.9 mbsf (Core 7X was empty). Core 9X took 2 h to advance 1.2 m, recovering 1.18 m of basalt (Figure F10). The slow rate of penetration was partly caused by the BHA being mostly above the seafloor, limiting the weight that could be applied safely. Cores 1H–9X recovered 45.4 m (93%). At 2245 h, we stopped coring to prepare for the transit to Reykjavík. We raised the drill bit, clearing the seafloor at 2355 h on 12 May and reaching the rig floor at 1150 h on 13 May, ending operations in Hole U1561A.

From 1230 to 1730 h, we deployed the subsea camera to 4881 mbsl, without the drill pipe, to detorque the camera's umbilical cable. This was done because the cable had wrapped around the drill pipe up to eight times during a deployment at Site U1556, and any residual twisting could damage the cable. While the camera was being lowered and raised back, the ship was secured for transit. We raised the thrusters, and at 1806 h we began the sea passage to Reykjavík. The transit took 22.6 days at an average speed of 10.6 kt.

#### 5.5.3. Principal results

The sediment/basalt contact in Hole U1561A is at 46.2 mbsf, and it is a sharp transition. We did not expect to reach basalt at 46.2 mbsf because the main basement seismic reflector is at ~126 mbsf at this site location, as estimated from seismic data. We do not yet know the reason for this discrepancy, nor for the differing estimates of seafloor depth between the seabed seismic reflection (4857 mbsl), the 12.5 kHz PDR reflection (4963.1 mbsl), and the mudline depth (4909.5 mbsl).

Cores 395E-U1561A-1H through 9X were measured on the WR and split-core track systems. Sections from Cores 8X and 9X, containing basalt (Figure F10), were measured on the WR tracks but were not split and were instead preserved in nitrogen gas-flushed bags for description and analysis during Expeditions 390 and 393. Core catcher samples from Cores 1H–6H were collected for postexpedition biostratigraphic dating. We collected one sample per core for headspace gas analy-

sis as well as 1 or 2 WR samples per core for chemical analysis of IW. The squeezed sediments from the IW samples were measured on the carbonate coulometer and XRD instruments. No systematic core description took place during Expedition 395E.

The sediment is red-brown clay from the seafloor to 22.5 mbsf (<1% calcium carbonate) and carbonate ooze from 22.5 to 46.2 mbsf (81–90 wt% calcium carbonate) (Figure F9). This change in lithology is reflected in the magnetic susceptibility and NGR data, which shift from relatively high values above 22.5 mbsf to lower values below as a result of the higher contents of terrigenous sediment in the red-brown clay. Some paleomagnetic reversals are evident in the SRM data, but not as many as would be expected if sediment had been continuously deposited at this site since the crust formed ~61.2 Ma, indicating that there are discontinuities or intervals of condensed sedimentation in the succession.

Preliminary analysis of the IW chemistry data shows that sulfate decreases slightly from 29.6 mM in the top core sample to ~26.5 mM for samples below ~20 mbsf. Ammonium has more variability, ranging from 12  $\mu$ M in the top sample to 62  $\mu$ M deeper in the hole. Most dissolved element profiles have some downhole structure but over narrow concentration ranges; for example, magnesium varies between 52.7 mM in the shallowest sample to 48.5 mM in the deepest sample. These results suggest that diagenetic processes at Site U1561 are slow, which is consistent with this site's open-ocean location and low organic matter input.

## 5.6. Transit and end of expedition

The transit north to Reykjavík began on 13 May 2021 at 1806 h and ended on 5 June at 0700 h when the pilot boarded (Figures F6, F7). The transit took 22.6 days at an average speed of 10.6 kt. The first line was ashore at 0818 h on 13 May, marking the end of Expedition 395E and the start of Expedition 395C.

# 6. Preliminary scientific assessment

The primary goal of Expedition 395E was to complete casing and reentry system installations for the South Atlantic Transect that were started during Expedition 390C and in preparation for Expeditions 390 and 393. Secondary goals included coring the sediment column and a few meters into basement with the APC/XCB coring system and analyzing cored material for ephemeral properties. Site U1560 was the first site of the expedition on the second-youngest crust (~15.2 Ma) of the transect, where we cored to basement and installed a reentry system. The operations plan was then adjusted to omit operations at Site SATL-33B, the site located on 30.6 Ma crust, because the expedition lost operations time when the ship departed from Cape Town, South Africa, 4 days later than planned and because calm sea states were forecast for Site U1557, which were essential for casing installation at that deepwater site. After completing the reentry systems at Sites U1557 and U1556, 2.5 days remained before the ship had to begin the transit to Iceland, and we used this time to core to basement at nearby alternate Site U1561. With the long transits, Expedition 395E had ~20 days of operational time along the SAT (Figures F6, F7; Table T2). Figure F8 shows work completed at SAT sites in addition to the remaining operational objectives to be accomplished during future SAT expeditions.

## 6.1. Operational considerations

During Expedition 390C, we found that it was not possible to release casing with the Dril-Quip system when the casing shoe was in basement rocks in Holes U1558B and U1558C, but the system released casing without difficulty when the casing shoe was positioned in sediment in Holes U1557D, U1558D, and U1559B. After Expedition 390C, it was recommended that for future endeavors involving installation of casing into basement, either a HRT reentry system should be used or the hole should be fully drilled out beyond the intended depth of the casing shoe prior to casing installation. Installing the casing shoe in basement is desirable because it helps to make a more stable hole for deep drilling where the top of basement is rubbly and unstable. Also, when the base of casing is in sediment and a lot of drilling fluid is pumped to remove cuttings, a washout

can develop, which can make it difficult to run logging tools into basement. For these reasons, we aimed to case into basement during Expedition 395E.

We used a HRT to release casing in Holes U1560B and U1556B during Expedition 395E. In Hole U1557D, the reentry cone and 60 m of 16 inch casing installed during Expedition 390C was compatible with Dril-Quip but not HRT, so this hole was first drilled out to 10 m into basement with a 14 inch bit, and then the 10½ inch casing was deployed to 5 m into basement without problems. In Hole U1560B, although we drilled to 2 m below the anticipated depth to basement, based on the depth it was found during coring operations in Hole U1560A, local seafloor topography meant that the casing shoe remained a small height (probably less than ~2 m) above basement. The gap between casing and basement was likely to have been filled when the bottom of casing was cemented.

In the cored holes at Sites U1560 and U1561, the XCB coring system with a PDC cutting shoe was used to advance 2–3 m into basalt. Similar to Expedition 390C, the PDC cutting shoe again performed very well.

In Hole U1561A, there were large differences between the anticipated and the actual seafloor and basement depths. The seafloor depth of 4909.5 mbsl (mudline) was 52.5 m deeper than the depth based on the seabed seismic reflection (4857 mbsl), and 53.6 m shallower than the depth based on the 12.5 kHz PDR reflection (4963.1 mbsl). Basalt was encountered at 46.2 mbsf in Hole U1561A, compared to the basement seismic reflector at ~126 mbsf at this site location.

**Table T2.** Expedition 395E site summary. APC = advanced piston corer, XCB = extended core barrel. NA = not applicable.

Hole	Latitude	Longitude	Water depth (m)	Total penetration (m)	Drilled interval (m)	Cored interval (m)	Core recovered (m)	Recovery (%)	Total cores (N)	APC cores (N)	XCB cores (N)
U1556B	30°56.5244'S	26°41.9472'W	5001.8	286.2	NA	NA	NA	0.00	0	0	0
			Site U1556 totals:	286.2	NA	NA	NA		0	0	0
U1557D	30°56.4651'S	26°37.7892'W	5010.7	576.6	516.6	NA	NA	0.00	0	0	0
			Site U1557 totals:	576.6	516.6	NA	NA		0	0	0
U1560A	30°24.2064'S	16°55.3718'W	3723.7	122.5	0.0	122.5	119.04	97.18	16	11	5
U1560B	30°24.2057'S	16°55.3702'W	3723.7	122.0	NA	NA	NA	0.00	0	0	0
			Site U1560 totals:	122.0	NA	122.5	119.04	97.18	16	11	5
U1561A	30°43.2902'S	26°41.7162'W	4909.5	48.9	0.0	48.9	45.41	92.86	9	6	3
U1561B	30°43.2902'S	26°41.7162'W	4909.5	9.5	0.0	9.5	9.63	101.37	1	1	0
U1561C	30°43.2902'S	26°41.7162'W	4909.5	9.5	0.0	9.5	10.20	107.37	1	1	0
			Site U1561 totals:	67.9		67.9	65.24		11	8	3
			Expedition totals:	2160.0	516.6	190.4	184.28		27	19	8

Hole	Start date (2021)	Start time UTC (h)	End date (2021)	End time UTC (h)	Time on hole (h)	Time on hole (days)	Comment
U1556B	5 May	0630	11 May	0000	137.52 137.52	5.73 5.73	Reentry system
U1557D	29 Apr	2215	5 May	0630	128.25 128.25	5.34 5.34	Reentry system
U1560A	22 Apr	0230	24 Apr	1515	60.72	2.53	
U1560B	24 Apr	1515	28 Apr	0000	80.64 141.36	3.36 5.89	Reentry system
U1561A	11 May	0345	11 May	2125	18.00	0.75	
U1561B	11 May	2225	11 May	2325	1.00	0.04	
U1561C	11 May	2325	13 May	2345	48.00 67.00	2.00 2.79	
					474.13	19.76	

## 6.2. Preliminary assessment of scientific objectives

Sediment and basalt were recovered at Sites U1560 and U1561 during Expedition 395E. Preliminary assessment of these cores was limited because no scientists were aboard, and the cores will be returned to *JOIDES Resolution* for visual core description during Expeditions 390 and 393. However, core images and physical property, paleomagnetic, and pore water geochemical data were collected during Expedition 395E and are briefly described here.

Site U1560 lies on 15.2 Ma crust at a water depth of 3723.7 m. The sediment is predominantly carbonate ooze (Figure F9) that ranges from 81 to 95 wt% calcium carbonate. Generally low values of magnetic susceptibility and NGR reflect the low terrigenous content of the carbonate ooze, and 10 m to submeter-scale variations in these physical property values reflect variations in terrigenous sediment content. Paleomagnetic reversals are evident in the SRM data, and a preliminary assessment of the reversal stratigraphy suggests that sedimentation was near-continuous at this site after the crust formed ~15 Ma. The magnetostratigraphic record will be refined after data from further holes are combined to make a complete stratigraphic splice during Expedition 390 or 393.

The sediment/basement contact in Hole U1560A is a sharp transition at 120.1 mbsf. The contact was deeper than originally estimated from seismic data (104 mbsf) but similar to what was expected from the basement depths cored during Expedition 390C. The basement depth in cased Hole U1560B is slightly deeper than in Hole U1560A, but the exact depth in Hole U1560B remains to be determined by drilling and logging during Expedition 390 or 393.

Preliminary analysis of IW chemistry data shows that sulfate has a flat profile, varying between 27.4 and 28.8 mM. Ammonium has more variability, ranging from 3  $\mu$ M near the top of the hole to 40  $\mu$ M near its base. Most dissolved element profiles have some downhole structure but over narrow concentration ranges; for example, magnesium varies between 49.7 and 52.5 mM. Headspace methane measurements were all below the detection limit. These results suggest that diagenetic processes at Site U1560 are slow, which is consistent with this site's open-ocean location and low organic matter input.

Site U1561 lies on ~61.2 Ma crust at a water depth of 4909.5 m. The sediment is red-brown clay from the seafloor to 22.5 mbsf (<1% calcium carbonate) and carbonate ooze from 22.5 to 46.2 mbsf (81–90 wt% calcium carbonate) (Figure F9). This change in lithology is reflected in the magnetic susceptibility and NGR data, which shift from relatively high values above 22.5 mbsf to lower values below as a result of the higher contents of terrigenous sediment in the red-brown clay. Some paleomagnetic reversals are evident in the SRM data, but not as many as would be expected if sediment had been continuously deposited at this site since the crust formed ~61.2 Ma, indicating that there are discontinuities or intervals of condensed sedimentation in the succession.

The sediment/basalt contact in Hole U1561A is at 46.2 mbsf, and it is a sharp transition. We did not expect to reach basalt at 46.2 mbsf because the main basement seismic reflector is at ~126 mbsf at this site location, as estimated from seismic data. We do not yet know the reason for this discrepancy, nor for the differing estimates of seafloor depth between the seabed seismic reflection (4857 mbsl), the 12.5 kHz PDR reflection (4963.1 mbsl), and the mudline depth (4909.5 mbsl).

Preliminary analysis of the IW chemistry data shows that sulfate decreases slightly from 29.6 mM in the top core sample to ~26.5 mM for the samples below ~20 mbsf. Ammonium has more variability, ranging from 12  $\mu$ M in the top to 62  $\mu$ M deeper in the hole. Most dissolved element profiles have some downhole structure but over narrow concentration ranges; for example, magnesium varies between 52.7 mM in the shallowest sample to 48.5 mM in the deepest sample. These results suggest that diagenetic processes at Site U1561 are slow, which is consistent with this site's open-ocean location and low organic matter input.

## 7. Outreach

No Onboard Outreach Officer sailed during Expedition 395E. Limited social media posts were made via the *JOIDES Resolution* Facebook and Twitter accounts.

## References

Alt, J.C., and Teagle, D.A.H., 1999. The uptake of carbon during alteration of ocean crust. *Geochimica et Cosmochimica Acta*, 63(10):1527–1535. [https://doi.org/10.1016/S0016-7037\(99\)00123-4](https://doi.org/10.1016/S0016-7037(99)00123-4)

Anderson, R.N., Honnorez, J., Becker, K., et al., 1985. Initial Reports of the Deep Sea Drilling Project, 83: Washington, DC (U.S. Government Printing Office). <https://doi.org/10.2973/dsdp.proc.83.1985>

Bach, W., and Edwards, K.J., 2003. Iron and sulfide oxidation within the basaltic ocean crust; implications for chemolithoautotrophic microbial biomass production. *Geochimica et Cosmochimica Acta*, 67(20):3871–3887. [https://doi.org/10.1016/S0016-7037\(03\)00304-1](https://doi.org/10.1016/S0016-7037(03)00304-1)

Barker, P.F., and Thomas, E., 2004. Origin, signature and palaeoclimatic influence of the Antarctic Circumpolar Current. *Earth-Science Reviews*, 66(1):143. <https://doi.org/10.1016/j.earscirev.2003.10.003>

Barrera, E., Savin, S.M., Thomas, E., and Jones, C.E., 1997. Evidence for thermohaline-circulation reversals controlled by sea-level change in the latest Cretaceous. *Geology*, 25(8):715–718. [https://doi.org/10.1130/0091-7613\(1997\)025<0715:EFTCRC>2.3.CO;2](https://doi.org/10.1130/0091-7613(1997)025<0715:EFTCRC>2.3.CO;2)

Berner, R.A., Lasaga, A.C., and Garrels, R.M., 1983. The carbonate-silicate geochemical cycle and its effect on atmospheric carbon dioxide over the past 100 million years. *American Journal of Science*, 283(7):641–683. <https://doi.org/10.2475/ajs.283.7.641>

Billups, K., 2002. Late Miocene through early Pliocene deep water circulation and climate change viewed from the sub-Antarctic South Atlantic. *Palaeogeography, Palaeoclimatology, Palaeoecology*, 185(3):287–307. [https://doi.org/10.1016/S0031-0182\(02\)00340-1](https://doi.org/10.1016/S0031-0182(02)00340-1)

Bohaty, S.M., Zachos, J.C., Florindo, F., and Delaney, M.L., 2009. Coupled greenhouse warming and deep-sea acidification in the middle Eocene. *Paleoceanography and Paleoclimatology*, 24(2):PA2207. <https://doi.org/10.1029/2008PA001676>

Borrelli, C., Cramer, B.S., and Katz, M.E., 2014. Bipolar Atlantic deepwater circulation in the middle-late Eocene: effects of Southern Ocean gateway openings. *Paleoceanography and Paleoclimatology*, 29(4):308–327. <https://doi.org/10.1002/2012PA002444>

Broecker, W.S., 1991. The great ocean conveyor. *Oceanography*, 4(2):79–89. <http://www.jstor.org/stable/43924572>

Cande, S.C., and Kent, D.V., 1995. Revised calibration of the geomagnetic polarity timescale for the Late Cretaceous and Cenozoic. *Journal of Geophysical Research*, 100:6093–6095. <https://doi.org/10.1029/94JB03098>

Coggon, R.M., Christeson, G.L., Sylvan, J.B., Teagle, D.A.H., Estes, E., Williams, T., and Alvarez Zarikian, C.A., 2020. Expedition 390/393 Scientific Prospectus: The South Atlantic Transect. International Ocean Discovery Program. <https://doi.org/10.14379/iodp.sp.390393.2020>

Coggon, R.M., and Teagle, D.A.H., 2011. Hydrothermal calcium-carbonate veins reveal past ocean chemistry. *TrAC Trends in Analytical Chemistry*, 30(8):1252–1268. <https://doi.org/10.1016/j.trac.2011.02.011>

Coggon, R.M., Teagle, D.A.H., Cooper, M.J., and Vanko, D.A., 2004. Linking basement carbonate vein compositions to porewater geochemistry across the eastern flank of the Juan de Fuca Ridge, ODP Leg 168. *Earth and Planetary Science Letters*, 219(1):111–128. [https://doi.org/10.1016/S0012-821X\(03\)00697-6](https://doi.org/10.1016/S0012-821X(03)00697-6)

Coggon, R.M., Teagle, D.A.H., Smith-Duque, C.E., Alt, J.C., and Cooper, M.J., 2010. Reconstructing past seawater Mg/Ca and Sr/Ca from mid-ocean ridge flank calcium carbonate veins. *Science*, 327(5969):1114–1117. <https://doi.org/10.1126/science.1182252>

Cramer, B.S., Toggweiler, J.R., Wright, J.D., Katz, M.E., and Miller, K.G., 2009. Ocean overturning since the Late Cretaceous: inferences from a new benthic foraminiferal isotope compilation. *Paleoceanography and Paleoclimatology*, 24(4):PA4216. <https://doi.org/10.1029/2008PA001683>

Davis, A.C., Bickle, M.J., and Teagle, D.A.H., 2003. Imbalance in the oceanic strontium budget. *Earth and Planetary Science Letters*, 211(1):173–187. [https://doi.org/10.1016/S0012-821X\(03\)00191-2](https://doi.org/10.1016/S0012-821X(03)00191-2)

Devey, C., 2014. SoMARTHerm: The Mid-Atlantic Ridge 13–33°S - Cruise No. MSM25 - January 24–March 5, 2013 - Cape Town (South Africa) - Mindelo (Cape Verde). DFG Senate Commission for Oceanography. [https://doi.org/10.2312/cr\\_msm25](https://doi.org/10.2312/cr_msm25)

D'Hondt, S., Inagaki, F., Alvarez Zarikian, C., Abrams, L.J., Dubois, N., Engelhardt, T., Evans, H., Ferdelman, T., Gribsholt, B., Harris, R.N., Hoppie, B.W., Hyun, J.-H., Kallmeyer, J., Kim, J., Lynch, J.E., McKinley, C.C., Mitsunobu, S., Morono, Y., Murray, R.W., Pockalny, R., Sauvage, J., Shimono, T., Shiraishi, F., Smith, D.C., Smith-Duque, C.E., Spivack, A.J., Steinsbu, B.O., Suzuki, Y., Szpak, M., Toffin, L., Uramoto, G., Yamaguchi, Y.T., Zhang, G.-I., Zhang, X.-H., and Ziebis, W., 2015. Presence of oxygen and aerobic communities from sea floor to basement in deep-sea sediments. *Nature Geoscience*, 8(4):299–304. <https://doi.org/10.1038/NGEO2387>

Dickens, G.R., Castillo, M.M., and Walker, J.C.G., 1997. A blast of gas in the latest Paleocene: simulating first-order effects of massive dissociation of oceanic methane hydrate. *Geology*, 25(3):259–262. [https://doi.org/10.1130/0091-7613\(1997\)025%3C0259:ABOGIT%3E2.3.CO;2](https://doi.org/10.1130/0091-7613(1997)025%3C0259:ABOGIT%3E2.3.CO;2)

Engelen, B., Ziegelmüller, K., Wolf, L., Köpke, B., Gittel, A., Cypionka, H., Treude, T., Nakagawa, S., Inagaki, L., Lever, M.A., and Steinsbu, B.O., 2008. Fluids from the oceanic crust support microbial activities within the deep biosphere. *Geomicrobiology Journal*, 25(1):56–66. <https://doi.org/10.1080/01490450701829006>

Estep, J., Reece, R., Kardell, D.A., Christeson, G.L., and Carlson, R.L., 2019. Seismic Layer 2A: evolution and thickness from 0- to 70-Ma crust in the slow-intermediate spreading South Atlantic. *Journal of Geophysical Research: Solid Earth*, 124(8):7633–7651. <https://doi.org/10.1029/2019JB017302>

Estes, E.R., Williams, T., Midgley, S., Coggon, R.M., Sylvan, J.B., Christeson, G.L., Teagle, D.A.H., and the Expedition 390C Scientists, 2021. Expedition 390C Preliminary Report: South Atlantic Transect Reentry Systems. *International Ocean Discovery Program*. <https://doi.org/10.14379/iodp.pr.390C.2021>

Expedition 301 Scientists, 2005. Expedition 301 summary. In Fisher, A.T., Urabe, T., Klaus, A., and the Expedition 301 Scientists, *Proceedings of the Integrated Ocean Drilling Program, 301: College Station, TX (Integrated Ocean Drilling Program Management International, Inc.)*. <https://doi.org/10.2204/iodp.proc.301.101.2005>

Expedition 309/312 Scientists, 2006. Expedition 309/312 summary. In Teagle, D.A.H., Alt, J.C., Umino, S., Miyashita, S., Banerjee, N.R., Wilson, D.S., and the Expedition 309/312 Scientists (Eds.), *Proceedings of the Integrated Ocean Drilling Program, 309/312: Washington, DC (Integrated Ocean Drilling Program Management International, Inc.)*. <https://doi.org/10.2204/iodp.proc.309312.101.2006>

Expedition 327 Scientists, 2011. Expedition 327 summary. In Fisher, A.T., Tsuji, T., Petronotis, K., and the Expedition 327 Scientists, *Proceedings of the Integrated Ocean Drilling Program, 327: Tokyo (Integrated Ocean Drilling Program Management International, Inc.)*. <https://doi.org/10.2204/iodp.proc.327.101.2011>

Expedition 329 Scientists, 2011. Expedition 329 summary. In D'Hondt, S., Inagaki, F., Alvarez Zarikian, C.A., and the Expedition 329 Scientists, *Proceedings of the Integrated Ocean Drilling Program, 329: Tokyo (Integrated Ocean Drilling Program Management International, Inc.)*. <https://doi.org/10.2204/iodp.proc.329.101.2011>

Expedition 330 Scientists, 2012. Expedition 330 summary. In Koppers, A.A.P., Yamazaki, T., Geldmacher, J., and the Expedition 330 Scientists, *Proceedings of the Integrated Ocean Drilling Program, 330: Tokyo (Integrated Ocean Drilling Program Management International, Inc.)*. <https://doi.org/10.2204/iodp.proc.330.101.2012>

Expedition 335 Scientists, 2012. Expedition 335 summary. In Teagle, D.A.H., Ildefonse, B., Blum, P., and the Expedition 335 Scientists, *Proceedings of the Integrated Ocean Drilling Program, 335: Tokyo (Integrated Ocean Drilling Program Management International, Inc.)*. <https://doi.org/10.2204/iodp.proc.335.101.2012>

Expedition 336 Scientists, 2012. Expedition 336 summary. In Edwards, K.J., Bach, W., Klaus, A., and the Expedition 336 Scientists (Eds.), *Proceedings of the Integrated Ocean Drilling Program, 336: Tokyo (Integrated Ocean Drilling Program Management International, Inc.)*. <https://doi.org/10.2204/iodp.proc.336.101.2012>

Frank, T.D., and Arthur, M.A., 1999. Tectonic forcings of Mastrichtian ocean-climate evolution. *Paleoceanography and Paleoclimatology*, 14(2):103–117. <https://doi.org/10.1029/1998PA900017>

Gillis, K.M., and Coogan, L.A., 2011. Secular variation in carbon uptake into the ocean crust. *Earth and Planetary Science Letters*, 302(3):385–392. <https://doi.org/10.1016/j.epsl.2010.12.030>

Inagaki, F., Nunoura, T., Nakagawa, S., Teske, A., Lever, M., Lauer, A., Suzuki, M., Takai, K., Delwiche, M., Colwell, F.S., Nealson, K.H., Horikoshi, K., D'Hondt, S., and Jørgensen, B.B., 2006. Biogeographical distribution and diversity of microbes in methane hydrate-bearing deep marine sediments on the Pacific Ocean margin. *Proceedings of the National Academy of Sciences of the United States of America*, 103(8):2815–2820. <https://doi.org/10.1073/pnas.0511033103>

Inagaki, F., and Orphan, V., 2014. Exploration of subseafloor life and the biosphere through IODP (2003–2013). In Stein, R., Blackman, Donna K., Inagaki, Fumio, and Larsen, Hans-Christian (Eds.), *Developments in Marine Geology (Volume 7): A Decade of Science Achieved by the Integrated Ocean Drilling Program (IODP)*. R. Stein (Series Ed.): 39–63. <https://doi.org/10.1016/B978-0-444-62617-2.00002-5>

Jungbluth, S.P., Grote, J., Lin, H.-T., Cowen, J.P., and Rappe, M.S., 2013. Microbial diversity within basement fluids of the sediment-buried Juan de Fuca Ridge flank. *The ISME Journal*, 7(1):161–172. <https://doi.org/10.1038/ismej.2012.73>

Kallmeyer, J., Pockalny, R., Adhikari, R.R., Smith, D.C., and D'Hondt, S., 2012. Global distribution of microbial abundance and biomass in subseafloor sediment. *Proceedings of the National Academy of Sciences of the United States of America*, 109(40):16213–16216. <https://doi.org/10.1073/pnas.1203849109>

Kardell, D.A., Christeson, G.L., Estep, J.D., Reece, R.S., and Carlson, R.L., 2019. Long-lasting evolution of Layer 2A in the western South Atlantic: evidence for low-temperature hydrothermal circulation in old oceanic crust. *Journal of Geophysical Research: Solid Earth*, 124(3):2252–2273. <https://doi.org/10.1029/2018JB016925>

Katz, M.E., Cramer, B.S., Toggweiler, J.R., Esmay, G., Liu, C., Miller, K.G., Rosenthal, Y., Wade, B.S., and Wright, J.D., 2011. Impact of Antarctic Circumpolar Current development on late Paleogene ocean structure. *Science*, 332(6033):1076–1079. <https://doi.org/10.1126/science.1202122>

Kennett, J.P., and Stott, L.D., 1990. Proteus and proto-oceanus: ancestral Paleogene oceans as revealed from Antarctic stable isotopic results; ODP Leg 113. In Barker, P.F., Kennett, J.P., et al. (Eds.), *Proceedings of the Ocean Drilling Program, Scientific Results, 113: College Station, TX (Ocean Drilling Program)*, 865–880. <https://doi.org/10.2973/ODP.PROC.SR.113.188.1990>

Kennett, J.P., and Stott, L.D., 1991. Abrupt deep-sea warming, palaeoceanographic changes and benthic extinctions at the end of the Palaeocene. *Nature*, 353(6341):225–229. <https://doi.org/10.1038/353225a0>

Lee, H.J., Jeong, S.E., Kim, P.J., Madsen, E.L., and Jeon, C.O., 2015. High resolution depth distribution of bacteria, archaea, methanotrophs, and methanogens in the bulk and rhizosphere soils of a flooded rice paddy. *Frontiers in Microbiology*, 6:639. <https://doi.org/10.3389/fmicb.2015.00639>

Lever, M.A., Rogers, K.L., Lloyd, K.G., Overmann, J., Schink, B., Thauer, R.K., Hoehler, T.M., and Jørgensen, B.B., 2015. Life under extreme energy limitation: a synthesis of laboratory- and field-based investigations. *FEMS Microbiology Reviews*, 39(5):688–728. <https://doi.org/10.1093/femsre/fuv020>

Lever, M.A., Rouxel, O., Alt, J.C., Shimizu, N., Ono, S., Coggon, R.M., Shanks, W.C., III, Lapham, L., Elvert, M., Prieto-Mollar, X., Hinrichs, K.-U., Inagaki, F., and Teske, A., 2013. Evidence for microbial carbon and sulfur cycling in deeply buried ridge flank basalt. *Science*, 339(6125):1305–1308. <https://doi.org/10.1126/science.1229240>

Lomstein, B.A., Langerhuus, A.T., D'Hondt, S., Jørgensen, B.B., and Spivack, A.J., 2012. Endospore abundance, microbial growth and necromass turnover in deep sub-seafloor sediment. *Nature*, 484(7392):101–104. <https://doi.org/10.1038/nature10905>

Mallows, C., and Searle, R.C., 2012. A geophysical study of oceanic core complexes and surrounding terrain, Mid-Atlantic Ridge 13°N–14°N. *Geochemistry, Geophysics, Geosystems*, 13(6):Q0AG08. <https://doi.org/10.1029/2012GC004075>

Mason, O.U., Nakagawa, T., Rosner, M., Van Nostrand, J.D., Zhou, J., Maruyama, A., Fisk, M.R., and Giovannoni, S.J., 2010. First investigation of the microbiology of the deepest layer of ocean crust. *PLoS One*, 5(11):e15399. <https://doi.org/10.1371/journal.pone.0015399>

Maus, S., Barckhausen, U., Berkenbosch, H., Bournas, N., Brozena, J., Childers, V., Dostaler, F., Fairhead, J.D., Finn, C., von Frese, R.R.B., Gaina, C., Golynsky, S., Kucks, R., Lühr, H., Milligan, P., Mogren, S., Müller, R.D., Olesen, O., Pilkington, M., Saltus, R., Schreckenberger, B., Thébault, E., and Tontini, F.C., 2009. EMAG2: a 2-arc min resolution Earth Magnetic Anomaly Grid compiled from satellite, airborne, and marine magnetic measurements. *Geochemistry, Geophysics, Geosystems*, 10(8):Q08005. <https://doi.org/10.1029/2009GC002471>

Mottl, M.J., 2003. Partitioning of energy and mass fluxes between mid-ocean axes and flanks at high and low temperature. In Halbech, P.E., Tunnicliffe, V. and Hein, J.R. (Eds.), *Energy and mass transfer in marine hydrothermal systems*: Berlin (Dahlem University Press), 271–286.

Müller, R.D., Sdrolias, M., Gaina, C., Steinberger, B., and Heine, C., 2008. Long-term sea-level fluctuations driven by ocean basin dynamics. *Science*, 319(5868):1357–1362. <https://doi.org/10.1126/science.1151540>

Norris, R.D., Wilson, P.A., Blum, P., Fehr, A., Agnini, C., Bornemann, A., Boulila, S., Bown, P.R., Cournede, C., Friedrich, O., Ghosh, A.K., Hollis, C.J., Hull, P.M., Jo, K., Junium, C.K., Kaneko, M., Liebrand, D., Lippert, P.C., Zhonghui, L., Matsui, H., Moriya, K., Nishi, H., Opdyke, B.N., Penman, D., Romans, B., Scher, H.D., Sexton, P., Takagi, H., Kirtland Turner, S., Whiteside, J.H., Yamaguchi, T., and Yamamoto, Y., 2014. Expedition 342 summary. In Norris, R.D., Wilson, P.A., Blum, P. and the Expedition 342 Scientists, *Proceedings of the Integrated Ocean Drilling Program*, 342: College Station, TX (Integrated Ocean Drilling Program). <https://doi.org/10.2204/iodp.proc.342.101.2014>

Orcutt, B.N., Bach, W., Becker, K., Fisher, A.T., Hentscher, M., Toner, B.M., Wheat, C.G., and Edwards, K.J., 2011. Colonization of subsurface microbial observatories deployed in young ocean crust. *The ISME Journal*, 5(4):692–703. <https://doi.org/10.1038/ismej.2010.157>

Orcutt, B.N., LaRowe, D.E., Lloyd, K.G., Mills, H., Orsi, W., Reese, B.K., Sauvage, J., Huber, J.A., and Amend, J., 2014. IODP Deep Biosphere Research Workshop report – a synthesis of recent investigations, and discussion of new research questions and drilling targets. *Scientific Drilling*, 17:61–66. <https://doi.org/10.5194/sd-17-61-2014>

Orcutt, B.N., Wheat, C.G., Rouxel, O., Hulme, S., Edwards, K.J., and Bach, W., 2013. Oxygen consumption rates in subseafloor basaltic crust derived from a reaction transport model. *Nature Communications*, 4:2539. <https://doi.org/10.1038/ncomms3539>

Pälike, H., Lyle, M.W., Nishi, H., Raffi, I., Ridgwell, A., Gamage, K., Klaus, A., Acton, G., Anderson, L., Backman, J., Baldauf, J., Beltran, C., Bohaty, S.M., Bown, P., Busch, W., Channell, J.E.T., Chun, C.O.J., Delaney, M., Dewangan, P., Dunkley Jones, T., Edgar, K.M., Evans, H., Fitch, P., Foster, G.L., Gussone, N., Hasegawa, H., Hathorne, E.C., Hayashi, H., Herrle, J.O., Holbourn, A., Hovan, S., Hyeong, K., Iijima, K., Ito, T., Kamikuri, S.-i., Kimoto, K., Kuroda, J., Leon-Rodriguez, L., Malinverno, A., Moore Jr, T.C., Murphy, B.H., Murphly, D.P., Nakamura, H., Ogane, K., Ohneiser, C., Richter, C., Robinson, R., Rohling, E.J., Romero, O., Sawada, K., Scher, H., Schneider, L., Slujs, A., Takata, H., Tian, J., Tsujimoto, A., Wade, B.S., Westerhold, T., Wilkens, R., Williams, T., Wilson, P.A., Yamamoto, Y., Yamamoto, S., Yamazaki, T., and Zeebe, R.E., 2012. A Cenozoic record of the equatorial Pacific carbonate compensation depth. *Nature*, 488(7413):609–614. <https://doi.org/10.1038/nature11360>

Palmer, M.R., and Edmond, J.M., 1989. The strontium isotope budget of the modern ocean. *Earth and Planetary Science Letters*, 92(1):11–26. [https://doi.org/10.1016/0012-821X\(89\)90017-4](https://doi.org/10.1016/0012-821X(89)90017-4)

Penrose Conference Participants, 1972. Penrose field conference on ophiolites. *Geotimes*, 17(12):24–25.

Perfit, M.R., and Chadwick, W.W., Jr., 1998. Magmatism at mid-ocean ridges: constraints from volcanological and geochemical investigations. In Buck, W.R., Delaney, J.A., Karson, J.A. and Lagabrielle, Y., *Faulting and Magmatism at Mid-Ocean Ridges*. *Geophysical Monograph*, 106:59–115. <https://doi.org/10.1029/GM106p0059>

Rausch, S., Böhm, F., Bach, W., Klügel, A., and Eisenhauer, A., 2013. Calcium carbonate veins in ocean crust record a threefold increase of seawater Mg/Ca in the past 30 million years. *Earth and Planetary Science Letters*, 362:215–224. <https://doi.org/10.1016/j.epsl.2012.12.005>

Reese, B.K., Zinke, L.A., Sobol, M.S., LaRowe, D.E., Orcutt, B.N., Zhang, X., Jaekel, U., Wang, F., Dittmar, T., Defforey, D., Tully, B., Paytan, A., Sylvan, J.B., Amend, J.P., Edwards, K.J., and Girguis, P., 2018. Nitrogen cycling of active bacteria within oligotrophic sediment of the Mid-Atlantic Ridge flank. *Geomicrobiology Journal*, 35(6):468–483. <https://doi.org/10.1080/01490451.2017.1392649>

Ryan, W.B.F., Carbotte, S.M., Coplan, J.O., O'Hara, S., Melkonian, A., Arko, R., Weissel, R.A., Ferrini, V., Goodwillie, A., Nitsche, F., Bonczkowski, J., and Zemsky, R., 2009. Global Multi-Resolution Topography synthesis. *Geochemistry, Geophysics, Geosystems*, 10(3):Q03014. <https://doi.org/10.1029/2008GC002332>

Santelli, C.M., Edgcomb, V.P., Bach, W., and Edwards, K.J., 2009. The diversity and abundance of bacteria inhabiting seafloor lavas positively correlate with rock alteration. *Environmental Microbiology*, 11(1):86–98. <https://doi.org/10.1111/j.1462-2920.2008.01743.x>

Scher, H.D., and Martin, E.E., 2006. Timing and climatic consequences of the opening of Drake Passage. *Science*, 312(5772):428–430. <https://doi.org/10.1126/science.1120044>

Schmid, F., Peters, M., Walter, M., Devey, C., Petersen, S., Yeo, I., Köhler, J., Jamieson, J.W., Walker, S., and Sültenfuß, J., 2019. Physico-chemical properties of newly discovered hydrothermal plumes above the southern Mid-Atlantic

Ridge (13°–33°S). Deep Sea Research Part I: Oceanographic Research Papers, 148:34–52.  
<https://doi.org/10.1016/j.dsr.2019.04.010>

Scientific Party, 1970. Introduction. In Maxwell, A.E., et al., Initial Reports of the Deep Sea Drilling Project, 3: Washington, DC (US Government Printing Office). <https://doi.org/10.2973/dsdp.proc.3.101.1970>

Shipboard Scientific Party, 1993. Explanatory notes. In Alt, J.C., Kinoshita, H., Stokking, L.B., et al., Proceedings of the Ocean Drilling Program, Initial Reports, 148: College Station, TX (Ocean Drilling Program).  
<https://doi.org/10.2973/odp.proc.ir.148.101.1993>

Shipboard Scientific Party, 1997. Introduction and summary: hydrothermal circulation in the oceanic crust and its consequences on the eastern flank of the Juan de Fuca Ridge. In Davies, E.E., Fisher, A.T., Firth, J.V., et al., Proceedings of the Ocean Drilling Program, Initial Reports, 168: College Station, TX (Ocean Drilling Program), 7–21.  
<https://doi.org/10.2973/odp.proc.ir.168.101.1997>

Shipboard Scientific Party, 2002. Leg 199 summary. In Lyle, M., Wilson, P.A., Janecek, T.R., et al., Proceedings of the Ocean Drilling Program, Initial Reports, 199: College Station, TX (Ocean Drilling Program).  
<https://doi.org/10.2973/odp.proc.ir.199.101.2002>

Shipboard Scientific Party, 2003. Leg 206 summary. In Wilson, D.S., Teagle, D.A.H., Acton, G.D., et al., Proceedings of the Ocean Drilling Program, Initial Reports, 206: College Station, TX (Ocean Drilling Program).  
<https://doi.org/10.2973/odp.proc.ir.206.101.2003>

Shipboard Scientific Party, 2004. Leg 208 summary. In Zachos, J.C., Kroon, D., Blum, P., et al., Proceedings of the Ocean Drilling Program, Initial Reports, 208: College Station, TX (Ocean Drilling Program).  
<https://doi.org/10.2973/odp.proc.ir.208.101.2004>

Spinelli, G.A., Giambalvo, E.R., and Fisher, A.T., 2004. Sediment permeability, distribution, and influence on fluxes in oceanic basement. In Davis, E.E., and Elderfield, H. (Eds.), *Hydrogeology of the Oceanic Lithosphere*: Cambridge, UK (Cambridge University Press), 151–188.

Staudigel, H., Hart, S.R., Schmincke, H.-U., and Smith, B.M., 1989. Cretaceous ocean crust at DSDP Sites 417 and 418: carbon uptake from weathering versus loss by magmatic outgassing. *Geochimica et Cosmochimica Acta*, 53(11):3091–3094. [https://doi.org/10.1016/0016-7037\(89\)90189-0](https://doi.org/10.1016/0016-7037(89)90189-0)

Stein, C.A., and Stein, S., 1994. Constraints on hydrothermal heat flux through the oceanic lithosphere from global heat flow. *Journal of Geophysical Research: Solid Earth*, 99(B2):3081–3095. <https://doi.org/10.1029/93JB02222>

Stommel, H., 1961. Thermohaline convection with two stable regimes of flow. *Tellus*, 13(2):224–230.  
<https://doi.org/10.1111/j.2153-3490.1961.tb00079.x>

Sylvan, J.B., Hoffman, C.L., Momper, L.M., Toner, B.M., Amend, J.P., and Edwards, K.J., 2015. *Bacillus rigiliprofundii* sp. nov., an endospore-forming, Mn-oxidizing, moderately halophilic bacterium isolated from deep subseafloor basaltic crust. *International Journal of Systematic and Evolutionary Microbiology*, 65(6):1992–1998.  
<https://doi.org/10.1099/ijss.0.000211>

Thomas, D.J., Bralower, T.J., and Jones, C.E., 2003. Neodymium isotopic reconstruction of late Paleocene–early Eocene thermohaline circulation. *Earth and Planetary Science Letters*, 209(3):309–322.  
[https://doi.org/10.1016/S0012-821X\(03\)00096-7](https://doi.org/10.1016/S0012-821X(03)00096-7)

Tobin, H.J., Kinoshita, M., Ashi, J., Lallement, S., Kimura, G., Screamton, E.J., Thu, M.K., Masago, H., and Curewitz, D., 2009. NanTroSEIZE Stage 1 expeditions: introduction and synthesis of key results. In Kinoshita, M., Tobin, H., Ashi, J., Kimura, G., Lallement, S., Screamton, E.J., Curewitz, D., Masago, H., Moe, K.T., and the Expedition 314/315/316 Scientists, *Proceedings of the Integrated Ocean Drilling Program*, 314/315/316: Washington, DC (Integrated Ocean Drilling Program Management, Inc.).  
<https://doi.org/10.2204/iodp.proc.314315316.101.2009>

Tripathi, A., Backman, J., Elderfield, H., and Ferretti, P., 2005. Eocene bipolar glaciation associated with global carbon cycle changes. *Nature*, 436(7049):341–346. <https://doi.org/10.1038/nature03874>

Vance, D., Teagle, D.A.H., and Foster, G.L., 2009. Variable Quaternary chemical weathering fluxes and imbalances in marine geochemical budgets. *Nature*, 458(7237):493–496. <https://doi.org/10.1038/nature07828>

Wheat, C.G., and Fisher, A.T., 2008. Massive, low-temperature hydrothermal flow from a basaltic outcrop on 23 Ma seafloor of the Cocos Plate: chemical constraints and implications. *Geochemistry, Geophysics, Geosystems*, 9(12):Q12O14. <https://doi.org/10.1029/2008GC002136>

Wright, J.D., Miller, K.G., and Fairbanks, R.G., 1991. Evolution of modern deepwater circulation: evidence from the late Miocene Southern Ocean. *Paleoceanography and Paleoclimatology*, 6(2):275–290.  
<https://doi.org/10.1029/90PA02498>

Wright, J.D., Miller, K.G., and Fairbanks, R.G., 1992. Early and middle Miocene stable isotopes: implications for deep-water circulation and climate. *Paleoceanography and Paleoclimatology*, 7(3):357–389.  
<https://doi.org/10.1029/92PA00760>

Wunsch, C., 2002. What is the thermohaline circulation? *Science*, 298(5596):1179–1181.  
<https://doi.org/10.1126/science.1079329>

Zachos, J., Pagani, M., Sloan, L., Thomas, E., and Billups, K., 2001. Trends, rhythms, and aberrations in global climate 65 Ma to Present. *Science*, 292(5517):686–693. <https://doi.org/10.1126/science.1059412>

Zachos, J.C., Dickens, G.R., and Zeebe, R.E., 2008. An early Cenozoic perspective on greenhouse warming and carbon-cycle dynamics. *Nature*, 451(7176):279–283. <https://doi.org/10.1038/nature06588>

Zachos, J.C., Röhl, U., Schellenberg, S.A., Sluijs, A., Hodell, D.A., Kelly, D.C., Thomas, E., Nicolo, M., Raffi, I., Lourens, L.J., McCarren, H., and Kroon, D., 2005. Rapid acidification of the ocean during the Paleocene–Eocene Thermal Maximum. *Science*, 308(5728):1611–1615. <https://doi.org/10.1126/science.1109004>

Zeebe, R.E., Zachos, J.C., Caldeira, K., and Tyrrell, T., 2008. Oceans: carbon emissions and acidification. *Science*, 321(5885):51–52. <https://doi.org/10.1126/science.1159124>